

# Particle–Continuum Coupling and its Scaling Regimes: Theory and Applications

Luigi Delle Site,\* Matej Praprotnik, John B. Bell, and Rupert Klein

This work is motivated by the goal of designing simulation software for technical devices that, at their functional core, rely on atomistic-scale processes embedded in a larger-scale fluid environment. The core of the problem is the conceptual and technical approach for coupling particle and continuum representations of a fluid. The state of the art for key aspects including physical modeling, mathematical formalization, computational implementation, and applications, is discussed and organized in a consistent picture across the relevant physical regimes.

## 1. Introduction

Potential applications, where we are in the presence of atomistic-scale processes embedded in a larger-scale fluid environment, are, for example, the electrochemical surface processes and large-scale transport around “artificial leaves”<sup>[1]</sup> that turn sunlight into the chemically bound energy of suitable substances, or thermophoretic micro-swimmers.<sup>[2]</sup> Such applications involve non-equilibrium states sustained by persistent material, momentum, or energy fluxes. As reported, for example, by R. Schmitz,<sup>[3]</sup> while fluctuations in fluids are always present, non-equilibrium states

give rise to hydrodynamic fluctuations that are correlated across mesoscales. These scales are too large to be covered efficiently by atomistic molecular dynamics simulations. Atomistic detail is, however, of central interest in the cited applications, and in this report we discuss coupled molecular dynamics (MD)–fluctuating hydrodynamics (FHD) simulations as a potentially fruitful approach to capturing the pertinent scale interactions.

Key building blocks of the related developments that we will summarize and appraise in some detail below are i) finite volume FHD solvers following Bell, Donev, Garcia, Nonaka and colleagues<sup>[4]</sup> (see Section 2), ii) the “adaptive resolution simulation” (AdResS) approach that enables molecular dynamics simulations on limited size domains<sup>[5–7]</sup> (see Section 3), and iii) the recent mathematical formalization of open molecular systems by two of the authors<sup>[8]</sup> (see Section 4). In Section 5, we discuss scaling regimes and the rationale behind possible MD–FHD coupling strategies, finally, Section 6 is dedicated to the description of some representative examples, while Section 7 outlines future perspectives and summarizes our conclusions.

## 2. Fluid Dynamics on Meso-Scales

In this report we are interested in processes on meso-scales and how they couple to the microscale. By the notion of “meso-scale” we refer to processes involving particle numbers that are finite but too large to allow for atomistically resolved simulations. The present section summarizes alternative approaches to modeling this regime in the light of their potential for contributing to micro-to-mesoscale coupled simulations.


There are two principally different lines of development that aim at the meso-scales: Particle-based coarse-graining techniques maintain the model structure of interacting particles but associate one of their representative particles with many of the microscopic degrees of freedom. This yields a modeling system with a manageable number of particles while the modeling challenge is to design effective particle models that faithfully represent the dynamics and statistics of the microscopic system on larger scales, see Section 2.1.

The alternative approach treats meso-scale modeling from the continuum perspective by reconsidering the derivation of continuum fluid mechanics from microscopic particle dynamics. Such derivations have a long-standing history but remain a topic of intense research.<sup>[9–15]</sup> Consistently, albeit along different routes of analysis, continuum mechanical conservation laws for

L. Delle Site, R. Klein  
Freie Universität Berlin  
Institute of Mathematics  
Arnimallee 6, 14195, Berlin, Germany  
E-mail: luigi.dellesite@fu-berlin.de

M. Praprotnik  
Laboratory for Molecular Modeling  
National Institute of Chemistry  
SI-1001 Ljubljana, Slovenia & Department of Physics  
Faculty of Mathematics and Physics  
University of Ljubljana  
SI-1000 Ljubljana, Slovenia

J. B. Bell  
Lawrence Berkeley National Lab 1 Cyclotron Rd. Berkeley  
CA 94720, USA

 The ORCID identification number(s) for the author(s) of this article can be found under <https://doi.org/10.1002/adts.201900232>

The copyright line for this article was changed on 21 January 2021 after original online publication.

© 2020 The Authors. Advanced Theory and Simulations published by Wiley-VCH GmbH. This is an open access article under the terms of the Creative Commons Attribution-NonCommercial-NoDerivs License, which permits use and distribution in any medium, provided the original work is properly cited, the use is non-commercial and no modifications or adaptations are made.

DOI: 10.1002/adts.201900232

mass, momentum, and energy are obtained in the limit of large particle numbers from a more general model for the dynamics or statistics of the underlying many particle system. In addressing the meso-scales following this route one maintains the mass, momentum, and energy densities as the primary unknowns, while the modeling challenge is to upgrade the continuum representation with stochastic or memory terms that cover for deviations from the deterministic continuum limit equations, see Sections 2.2 and 2.3.

## 2.1. Coarse-Grained Molecular Dynamics and Particle-Based Fluid Models

### 2.1.1. Coarse-Grained Molecular Dynamics Models

Coarse-grained (CG) MD<sup>[16]</sup> aims at the efficient extension of atomistically detailed molecular dynamics to length and time scales otherwise inaccessible to the latter. The idea is to retain the principal model structure of MD but to utilize artificial particles and particle interactions that are specifically designed to reproduce important statistical properties of the atomistic counterparts of the considered systems. Typically, the detailed degrees of freedom of a group of molecules or of parts of a single complex molecule are collected into representative “coarse-grained” particles with a much lower number of internal degrees of freedom. Representative particles interact through effective potentials which, depending on the intended degree of model reduction, are custom-fitted such that selected statistical properties agree between the considered material and the CG MD model. Thus, these pair interactions are typically tuned so that equilibrium statistical properties, such as free energies, radial distribution functions, or their Fourier space counterparts, the structure factors, are reproduced.<sup>[17]</sup> The number of statistical characteristics that can be matched to those of the respective detailed model is generally limited (see e.g., refs. [18, 19] and references therein).

In the context of the present paper, such CG models represent an intermediate level of model reduction between atomistic MD and a continuum mechanical representation of fluid dynamics. Yet, because it is not clear that the large scale–many particle continuum limit of a given CG model will match that of the underlying atomistic model automatically, one must ensure that the particular statistical properties of the two systems that define the material parameters of the associated fluid are in agreement. Examples are the diffusivities and viscosities as defined by time autocorrelation functions according to the Green–Kubo formulae.<sup>[20,21]</sup> However, the fitting of statistical parameters at the level of time correlations is, to the best of the authors’ knowledge, today the exception rather than the rule. A numerical check done a posteriori may sometimes be employed to detect a capability of a CG model for reproducing certain time correlations that is not expected a priori on theoretical grounds.<sup>[22]</sup> For further discussion of the role of CG models in multiscale simulations involving atomistic–CG hybrid models see also Section 3 below.

### 2.1.2. Particle-Based Fluid Dynamics

It is possible, on the other hand, to directly design particle-based simulation models so as to reproduce the continuum mechan-

ics of a specific fluid with given material properties. Prominent examples are the Smooth Particle Hydrodynamics<sup>[23]</sup> (SPH) and Dissipative Particle Dynamics (DPD) models,<sup>[24]</sup> direct simulation Monte Carlo (DSMC) schemes,<sup>[25]</sup> Yserentant’s finite particle discretization of the compressible Euler equations,<sup>[26]</sup> and the Lattice Boltzmann method,<sup>[27]</sup> although the latter is based on a combination of grid- and particle-based modelling principles in contrast to the other grid-free schemes which work with interacting particles only. We note that, while DSMC was originally developed as a particle-based continuum solver for rarefied gases, when each DSMC particle represents a single molecule the DSMC model provides an accurate atomistic description of dilute gases.<sup>[28,29]</sup>

Particle-based fluid dynamics models are attractive for several reasons. They allow, for example, for the flexible and efficient representation of complex flow domain boundaries and they naturally include fluctuations about mean fluid dynamical flow states, although they can only approximate the details of the fluctuation statistics in general. Furthermore, their mathematical structure is close to that of atomistic and CG MD models which makes them an attractive option in the development of seamless multiscale simulation schemes that bridge between the atomistic and continuum fluid dynamical scales. Recent developments have shown, however, that grid-based FHD models, to be described in more detail in Section 2.3 below, are well capable of representing fluid dynamical length and time scales across a very wide range of scales, starting at grid resolutions for which a typical grid cell covers just tens to hundreds of molecules.<sup>[30,31]</sup> That being the case, and since atomistic MD simulations typically require at least this number of particles in a simulation, it seems justified to attempt a direct coupling between atomistic MD and FHD, thereby skipping the added complexity of intermediate CG MD or particle-based hydrodynamic models.

There is also evidence<sup>[32]</sup> that large distance tails of two-point velocity correlations get distorted in small-domain particle-based simulations but that these can be recovered in hybrid models that cover the large scales by grid-based FHD.

## 2.2. Single-Particle Distributions and the Boltzmann Equation

Ludwig Boltzmann<sup>[9]</sup> pioneered an approach that takes a detour via the single particle probability density. Considering spherical particles that interact only upon collision with each other and starting from the dynamics of the full many-particle system, he derives the famous Boltzmann equation for the probability density  $f(t, \mathbf{r}, \mathbf{v})$  of finding at time  $t$  and location  $\mathbf{r}$  a particle with given velocity  $\mathbf{v}$ . For a system with identical particles of mass  $M$ , one may define the continuum mechanical mass, momentum, and energy densities as statistical moments with respect to the velocity variable of that distribution, so that  $\rho(t, \mathbf{r}) = \langle Mf(t, \mathbf{r}, \mathbf{v}) \rangle_{\mathbf{v}}$ ,  $\rho \mathbf{v}(t, \mathbf{r}) = \langle M \mathbf{v} f(t, \mathbf{r}, \mathbf{v}) \rangle_{\mathbf{v}}$ , and  $\rho e(t, \mathbf{r}) = \langle M (\mathbf{v}^2/2) f(t, \mathbf{r}, \mathbf{v}) \rangle_{\mathbf{v}}$ , respectively. Depending on suitable choices of distinguished limits between particle numbers and length and time scales one can show rigorously that the evolution of statistical moments as determined by the Boltzmann equation is compatible with the compressible or incompressible Euler or Navier–Stokes equations. The time scale of validity of these limits depends on the particular regime considered and on smoothness properties

of the reference continuum solutions. Much of this scientific program has meanwhile been developed all the way to the level of rigorous mathematical theorems and proofs.<sup>[13–15]</sup>

In the present context, it is important to notice, however, that adoption of Boltzmann's equation as an intermediate model—located between the Liouville equation for the  $N$ -particle state space distribution on the one hand and the continuum mechanical conservation laws for the mass, momentum, and energy densities on the other hand—implies that only limited information regarding fluctuations of these fields remains available: One can assess local statistical quantities such as variances, skewnesses, etc., but to calculate, for example, space and time correlations, multi-point statistical information would be required.

More specifically, we note that  $f(t, \mathbf{r}, \mathbf{v})$  is the expected value (or marginal) of the full many-particle distribution with respect to the positions and velocities of all other particles in the system. That being so,  $f(t, \mathbf{r}, \mathbf{v})$  does describe the expected local densities of mass, momentum, and energy but any information about statistical deviations from these is by construction inaccessible to the Boltzmann approach. After all, deviations from, for example, the expected mass in a control volume require many particles to collude in populating or not populating that volume and the statistics of such an accumulation necessarily requires access to the many particle joint probability distribution. As discussed below in Section 4, however, the faithful coupling of atomistic microscale to effective mesoscale models requires the latter to provide accurate fluctuation information to the former. Otherwise, important system properties such as, for example, grand canonical fluctuation statistics, cannot be maintained in the coupled simulation. As a consequence, the Boltzmann theory has limited value as a starting point for developing micro-to-mesoscale hybrid models

### 2.3. Many-Particles, Projection Operators, and Fluctuating Hydrodynamics

An approach that is in this sense more general, but much less amenable to rigorous mathematical analysis so far, is the projection operator technique.<sup>[10,12,33,34]</sup> This technique has been employed in the construction of continuum fluid dynamics models that include stochastic noise terms to represent the influence of thermal fluctuations in many particle systems onto the continuum mechanical observables, that is, onto the mass, momentum, and energy densities.<sup>[11]</sup> The resulting “fluctuating hydrodynamics” equations generalize the linearized theory of Landau and Lifshitz.<sup>[35]</sup> Moreover, the projection operator technique is sufficiently general to also include memory effects that may arise in general coarse-graining procedures. For its generality and as it is the theoretical basis for continuum FHD models, we provide a more detailed overview of the technique in the following Subsections 2.3.1–2.3.6. Subsections 2.3.7 and 2.3.8 will then summarize the state of the art of thermodynamically faithful (reacting) FHD models.

#### 2.3.1. Time Evolution of State Space Distributions

Suppose  $\Omega$  and  $\mathbf{X} \in \Omega$  denote the state space and a particular state of a complex many-particle (Hamiltonian) dynamical sys-

tem, respectively, and that its dynamics is governed by  $\dot{\mathbf{X}} = \mathbf{R}(\mathbf{X})$ . More specifically, for an  $N$ -particle system we may think of  $\mathbf{X} = (\mathbf{p}_i, \mathbf{r}_i)_{i=1}^N$  to denote the collection of all particle momenta,  $\mathbf{p}_i$ , and positions,  $\mathbf{r}_i$ . The projection operator technique originates in non-equilibrium statistical mechanics. It takes the evolution equation of state space probability distributions,

$$f : \mathbb{R}^+ \times \Omega \rightarrow \mathbb{R}^+ \quad (t, \mathbf{X}) \mapsto f(t, \mathbf{X}), \quad \int_{\Omega} f(t, \mathbf{X}) d\mathbf{X} = 1 \quad (1)$$

where  $\mathbb{R}^+ = \{x \in \mathbb{R} \mid x \geq 0\}$ , that is, the Liouville equation,

$$\left( \frac{\partial}{\partial t} + \mathbf{R} \cdot \nabla_{\mathbf{X}} \right) f(t, \mathbf{X}) = 0 \quad (2)$$

as its point of departure. Equation (2) is a scalar linear advection equation for which  $\mathbf{R}(\mathbf{X})$  plays the role of the transport velocity. Given an initial distribution, so that  $f(0, \mathbf{X}) = f_0(\mathbf{X})$ , the Liouville equation is solved straightforwardly by the method of characteristics: The characteristic curves of (2) are defined by trajectories of the underlying dynamical system

$$\mathbf{X}(t) \equiv \Phi^t \mathbf{X}_0 \quad \text{which satisfy} \quad \frac{d\mathbf{X}}{dt} = \mathbf{R}(\mathbf{X}), \quad \mathbf{X}(0) = \mathbf{X}_0 \quad (3)$$

Then (2) states that the probability density  $f(t, \mathbf{X})$  is constant along the characteristic curves. The density at time  $t$  and state  $\mathbf{X}$  may therefore be evaluated by following the characteristic passing through  $\mathbf{X}$  backward in time to  $t = 0$  and evaluating the initial density  $f_0$  at that location,

$$f(t, \mathbf{X}) = f_0(\Phi^{-t} \mathbf{X}) \equiv (f_0 \circ \Phi^{-t})(\mathbf{X}) \quad (4)$$

where the  $\circ$ -symbol denotes function composition. The Liouville equation encodes the same information as the original Hamiltonian system. Its advantage for analytical purposes is its linearity, its disadvantage is that its unknown is a function of  $N^6$  state space coordinates, which makes its actual solution an arduous task.

Reasons to hope that this “curse of dimensionality” can be addressed come from the fact that the effective behavior of macroscopic (very) many particle systems are often described extremely well by the evolution of a rather small number of effective variables that are functions of time and physical space only. For instance, the dynamics of a homogeneous fluid is governed essentially by the conservation laws for mass, momentum, and total energy densities in the form of the Euler or Navier–Stokes equations. These constitute just five, albeit nonlinear, partial differential equations in merely three space dimensions and time.

#### 2.3.2. Liouville Operator

The projection operator approach aims to provide a systematic procedure for deriving such reduced dynamical systems from the Liouville equation. To this end, (2) is first cast in a form that emphasizes its linearity and turns out to be notationally convenient,

$$\frac{\partial f}{\partial t} = -\mathcal{L}f, \quad \text{where} \quad \mathcal{L} = \mathbf{R}(\mathbf{X}) \cdot \nabla_{\mathbf{X}} \quad (5)$$

Recall that  $\mathcal{L}$  is a linear operator because the argument  $\mathbf{X}$  of the advection velocity  $\mathbf{R}$  is an independent variable of the unknown function  $f(t, \mathbf{X})$ . Formally, given an initial distribution  $f(0, \mathbf{X}) = f_0(\mathbf{X})$ , the exact solution of the Liouville equation then reads

$$f(t, \mathbf{X}) = (e^{-t\mathcal{L}} f_0)(\mathbf{X}), \quad e^{-t\mathcal{L}} = \sum_{k=0}^{\infty} \frac{(-t)^k}{k!} \mathcal{L}^k \quad (6)$$

where the operator exponential is defined by its Taylor series as indicated. Going back to (4) above, we note that its action is readily identified as

$$f(t, \cdot) = (e^{-t\mathcal{L}} f_0)(\cdot) \equiv (f_0 \circ \Phi^{-t})(\cdot) \quad (7)$$

The Liouville operator also describes the time evolution of any physical observable  $\tilde{\mathbf{A}} : \Omega \rightarrow \Omega_A$

where  $\Omega_A \subseteq \mathbb{R}^m$  is a set of quantities that we can “observe” in the sense of experimental measurements. In fact, let

$$\mathbf{A}(t) = \tilde{\mathbf{A}}(\mathbf{X}(t)) = \tilde{\mathbf{A}}(\Phi^t \mathbf{X}_0) = (\tilde{\mathbf{A}} \circ \Phi^t)(\mathbf{X}_0) \quad (9)$$

denote the time evolution of measurements along the trajectory  $\Phi^t \mathbf{X}_0$  of our system starting from  $\mathbf{X}_0$ . Then, we see by comparison with (7) and (2) that there is a time dependent observation function (or operator)

$$\tilde{\mathbf{A}}_t : \Omega \rightarrow \Omega_A; \quad \mathbf{X}_0 \mapsto (\tilde{\mathbf{A}} \circ \Phi^t) \mathbf{X}_0 = (e^{t\mathcal{L}} \tilde{\mathbf{A}})(\mathbf{X}_0) \quad (10)$$

which, when evaluated at the initial state  $\mathbf{X}_0$  generates the observation at time  $t$  for the trajectory emerging from that state.

We note in passing that the change of perspective implied by  $\tilde{\mathbf{A}}(\mathbf{X}(t)) = \tilde{\mathbf{A}}_t(\mathbf{X}_0)$  corresponds to the equivalence of the Schrödinger and Heisenberg pictures in Quantum Mechanics. The former considers the observation operation to be given while the system’s state changes, the latter identifies a trajectory of the system with its initial state and associates the evolution of the observation with the observation operator itself. We also observe that (10) determines the evolution equation of the observables as

$$\frac{d}{dt} \mathbf{A}(t) = (\mathcal{L} \tilde{\mathbf{A}})(\mathbf{X}(t)) \quad (11)$$

### 2.3.3. The Statistics of Arbitrary Functions of Relevant Observables

Given that one can measure and is interested in merely a limited set of “relevant” observables of a many-particle system, the detailed information encoded in the state space probability density  $f$  from (1) is more than is needed or of interest in practice. Now, let  $\tilde{\mathbf{A}} = \{\tilde{\mathbf{A}}_1, \dots, \tilde{\mathbf{A}}_m\}$  for some  $m \in \mathbb{N} \cup \{\infty\}$  denote a finite or infinite set of such relevant observables as defined in (8). Then what is of interest in the sense of statistical mechanics is the probability density in the space  $\Omega_{\tilde{\mathbf{A}}}$  spanned by these observables, that is,

$$p : \mathbb{R}^+ \times \Omega_{\tilde{\mathbf{A}}} \rightarrow \mathbb{R}^+ \quad (t, \underline{\alpha}) \mapsto p(t, \underline{\alpha}), \quad \int_{\Omega_{\tilde{\mathbf{A}}}} p(t, \underline{\alpha}) d\underline{\alpha} = 1 \quad (12)$$

If we are given the detailed state space distribution,  $f$ , then the density in observable space is straightforwardly computed as

$$\begin{aligned} p(t, \underline{\alpha}) &= \int_{\Omega} \delta(\tilde{\mathbf{A}}(\mathbf{X}) - \underline{\alpha}) f(t, \mathbf{X}) d\mathbf{X} \\ &= \int_{\Omega} \delta(\tilde{\mathbf{A}}(\Phi^t \mathbf{X}_0) - \underline{\alpha}) f_0(\mathbf{X}_0) d\mathbf{X}_0 \end{aligned} \quad (13)$$

In the second expression, we have introduced a variable transformation that maps the state  $\mathbf{X}$  to the origin  $\mathbf{X}_0 = \Phi^{-t} \mathbf{X}$  of the trajectory that passes through  $\mathbf{X}$  at time  $t$ . From this representation it becomes clear that the time dependence of  $p(t, \underline{\alpha})$  is fully determined by that of the elementary distributions  $\delta(\tilde{\mathbf{A}}(\Phi^t \mathbf{X}_0) - \underline{\alpha})$  which we will address shortly.

Interestingly, the time evolution of any function of the observables, say  $g(\underline{\alpha})$ , is also determined entirely by that of the elementary distributions since

$$g(\mathbf{A}(t)) = g(\tilde{\mathbf{A}}(\mathbf{X}(t))) = \int_{\Omega_{\tilde{\mathbf{A}}}} g(\underline{\alpha}) \delta(\tilde{\mathbf{A}}(\Phi^t \mathbf{X}_0) - \underline{\alpha}) d\underline{\alpha} \quad (14)$$

Finally, the statistics of values of such functions is encoded by

$$\begin{aligned} p_g(t, \gamma) &= \int_{\Omega} \delta(g(\tilde{\mathbf{A}}(\mathbf{X})) - \gamma) f(t, \mathbf{X}) d\mathbf{X} \\ &= \int_{\Omega_A} \delta(g(\underline{\alpha}) - \gamma) \left[ \int_{\Omega} \delta(\tilde{\mathbf{A}}(\mathbf{X}) - \underline{\alpha}) f(t, \mathbf{X}) d\mathbf{X} \right] d\underline{\alpha} \\ &= \int_{\Omega_A} \delta(g(\underline{\alpha}) - \gamma) p(t, \underline{\alpha}) d\underline{\alpha}, \end{aligned} \quad (15)$$

and it is thus fully determined by the distribution  $p(t, \underline{\alpha})$  in the space of the relevant observables.

For these reasons, the time evolution of the elementary distributions  $\delta(\tilde{\mathbf{A}}(e^{t\mathcal{L}} \mathbf{X}_0) - \underline{\alpha})$  is of central interest in the projection operator approach.<sup>[10]</sup>

### 2.3.4. Projections

If all we can effectively measure in terms of the state of a system are the relevant observables  $\tilde{\mathbf{A}}$ , then it makes sense to separate the statistics of general state space functions  $F(\mathbf{X})$  into their conditional expectations on level sets of these observables, that is,

$$\langle F \rangle^{\underline{\alpha}} = \int_{\Omega} \frac{F(\mathbf{X})}{p(0, \underline{\alpha})} \delta(\tilde{\mathbf{A}}(\mathbf{X}) - \underline{\alpha}) f_0(\mathbf{X}) d\mathbf{X} \quad (16)$$

and their deviations from these. This gives rise to the projection operator  $\mathbb{P}$  which maps general state space functions to these expected values on the level sets of the relevant observables such that

$$\mathbb{P}F(\mathbf{X}) = \int_{\Omega_{\tilde{\mathbf{A}}}} \langle F \rangle^{\underline{\alpha}} \delta(\tilde{\mathbf{A}}(\mathbf{X}) - \underline{\alpha}) d\underline{\alpha} = \langle F \rangle^{\tilde{\mathbf{A}}(\mathbf{X})} \quad (17)$$

Obviously,  $\mathbb{P}\mathbb{P}F = \mathbb{P}F$ , that is, the operation is indeed a projection, and in the sequel we denote its complement by  $\mathbb{Q} = \mathbb{I} - \mathbb{P}$ .

### 2.3.5. Time Evolution of The Elementary Distributions

$$\delta(\tilde{\mathbf{A}}(\mathbf{X}(t)) - \underline{\alpha})$$

The last two sections have demonstrated that elementary distributions  $\delta(\tilde{\mathbf{A}}(e^{t\mathcal{L}}\mathbf{X}_0) - \underline{\alpha})$  play a central role in the model reduction process. Here we consider the time evolution of these elementary distributions closely following refs. [10, 33].

Equation (10) provides a compact description of the time evolution of any state space function along a trajectory that starts in some initial state  $\mathbf{X}_0$ . The elementary distributions are generalized state space functions as well with values in the set of Dirac- $\delta$  distributions in the space of observables. Thus, neglecting for this formal calculation the difficulty that these are singular distributions so that expressions involving their gradients w.r.t. the state variables can at best be defined in a weak sense, we have

$$\delta(\tilde{\mathbf{A}}(\mathbf{X}(t)) - \underline{\alpha}) = \delta(\tilde{\mathbf{A}}(\Phi^t\mathbf{X}_0) - \underline{\alpha}) = \left( e^{t\mathcal{L}}\delta(\tilde{\mathbf{A}}(\cdot) - \underline{\alpha}) \right)(\mathbf{X}_0) \quad (18)$$

To abbreviate the notation in the sequel we let<sup>[10,33]</sup>

$$\delta(\tilde{\mathbf{A}}(\mathbf{X}) - \underline{\alpha}) \equiv \Psi_{\underline{\alpha}}(\mathbf{X}) \quad (19)$$

and then (18) yields

$$\frac{\partial}{\partial t}\Psi_{\underline{\alpha}}(\mathbf{X}(t)) = \left( e^{t\mathcal{L}}\mathcal{L}\Psi_{\underline{\alpha}}(\cdot) \right)(\mathbf{X}_0) \quad (20)$$

The next goal is to utilize the projection operators  $\mathbb{P}$  and  $\mathbb{Q} = \mathbb{I} - \mathbb{P}$  to decompose the right hand side into terms that vary only between the level sets of the relevant observables, that is, terms for which a deterministic closure might be achievable, on the one hand, and terms with zero conditional average over these level sets, that is, terms not expressible in terms of the observables only, on the other hand. To this end the following identity comes handy,<sup>[33]</sup>

$$e^{t\mathcal{L}} = e^{t\mathcal{L}}\mathbb{P} + \int_0^t e^{s\mathcal{L}}\mathbb{P}\mathcal{L}\mathbb{Q}e^{(t-s)\mathcal{L}}ds + \mathbb{Q}e^{t\mathcal{L}}\mathbb{Q} \equiv \text{rhs}(t) \quad (21)$$

This identity is verified as follows: First, we observe that for  $t = 0$  both the left and right hand sides of the equation reduce to the identity. Second, we subtract  $e^{t\mathcal{L}}$  from both sides of the equation and take the time derivative of the resulting expressions. Observing that for any operator  $B$  for which the operator exponential exists we have  $\frac{d}{dt}e^{tB} = e^{tB}B$ , we find

$$\begin{aligned} \frac{\partial}{\partial t}(\text{rhs}(t) - e^{t\mathcal{L}}) &= -e^{t\mathcal{L}}\mathcal{L}\mathbb{Q} + e^{t\mathcal{L}}\mathbb{P}\mathcal{L}\mathbb{Q} \\ &+ \int_0^t e^{s\mathcal{L}}\mathbb{P}\mathcal{L}\mathbb{Q}e^{(t-s)\mathcal{L}}\mathcal{L}\mathbb{Q}ds + \mathbb{Q}e^{t\mathcal{L}}\mathcal{L}\mathbb{Q} \end{aligned} \quad (22a)$$

$$= (\text{rhs}(t) - e^{t\mathcal{L}})\mathcal{L}\mathbb{Q} \quad (22b)$$

Since  $(\text{rhs}(t) - e^{t\mathcal{L}})|_{t=0} = 0$  as pointed out above, (22) is indeed solved when (21) is satisfied for all  $t$ . Insertion of that identity in (20) yields

$$\begin{aligned} \frac{\partial}{\partial t}\Psi_{\underline{\alpha}}(\mathbf{X}(t)) &= \left( \left( e^{t\mathcal{L}}\mathbb{P}\mathcal{L}\Psi_{\underline{\alpha}}(\cdot) \right) \right. \\ &\left. + \int_0^t e^{s\mathcal{L}}\mathbb{P}\mathcal{L}\mathbb{Q}e^{(t-s)\mathcal{L}}\mathcal{L}\Psi_{\underline{\alpha}}(\cdot)ds + \mathbb{Q}e^{t\mathcal{L}}\mathcal{L}\Psi_{\underline{\alpha}}(\cdot) \right)(\mathbf{X}_0) \end{aligned} \quad (23)$$

$$= \mathbb{P}\mathcal{L}\Psi_{\underline{\alpha}}(\mathbf{X}(t))$$

$$+ \mathbb{P} \int_0^t \mathcal{L}\mathbb{Q}e^{(t-s)\mathcal{L}}\mathcal{L}\Psi_{\underline{\alpha}}(\mathbf{X}(s))ds + \mathbb{Q}e^{t\mathcal{L}}\mathcal{L}\Psi_{\underline{\alpha}}(\mathbf{X}_0) \quad (24)$$

The first two terms in this expression for the rate of change of the elementary distributions are projections onto the space of the relevant observables. That is, they can in principle be expressed as functions of the observables through appropriate closure formulae. The third term is not accessible this way for two reasons. First, it is itself in the orthogonal complement of the space of functions of the observables since the last operation involved in computing it is the projection onto this complement,  $\mathbb{Q}$ . Second, it involves the orthogonal dynamics induced by the operator  $\mathcal{L}\mathbb{Q}$ , that is, by the Liouville operator being applied only to the “complementary” part of its argument.

### 2.3.6. Finite Volume Averages as Observables

In the theory of compressible fluid dynamics, the conservation laws for mass, momentum, and energy play a central role. These methods keep grid cell averaged densities of these conserved quantities as the primary dependent variables which get updated in time by balances of suitable flux approximations across the grid cell faces. This way, conservative finite volume methods provide a natural link with derivations of the flow equations from the Boltzmann equation<sup>[14]</sup> as balances of statistical moments of the single-particle distribution function; they constitute the physical basis for the concept of weak solutions<sup>[36]</sup> which allows us to make mathematical sense of shock waves, contact discontinuities, and more general non-smooth solutions; and, in close correspondence with the latter, they motivate robust numerical discretizations in conservation form [37]. Moreover, many strategies for coupling particle-based and continuum mechanical descriptions of fluid motions rely on subdivisions of the flow domain into subregions with particle- and continuum representations and on matching the respective fluxes of mass, momentum, and energy across the respective interfaces (see Section 3 below). These observations motivate the following closer examination of the projection operator technique applied with finite volume averages of the fundamental conserved quantities as the underlying observables.

Español<sup>[11]</sup> provides an overview of the derivation of fluctuating hydrodynamics in just this framework. In doing so, he opts



for the second of the following two alternative paths established in the literature (see related discussions in ref. [33]):

1. Directly utilize the evolution Equation (23) for the elementary distributions  $\Psi_{\underline{\alpha}}(\mathbf{X}(t))$ , insert the definition  $\underline{\mathbf{A}}(t) = \tilde{\underline{\mathbf{A}}}(\mathbf{X}(t)) = \int_{\Omega_{\underline{\mathbf{A}}}} \delta(\mathbf{X}(t) - \underline{\alpha}) \underline{\alpha} d\underline{\alpha}$ , and make sense of the unclosed terms arising from the complementary projections  $\mathbb{Q} = \mathbb{I} - \mathbb{P}$  in the resulting expressions in deriving directly a Langevin-type equation for the observables.
2. Use (23) instead to establish the evolution equation for the observable space density,  $p(t, \underline{\alpha})$ , from (13), utilize Zubarev & Morozov's<sup>[38]</sup> arguments for the closure of said terms within this framework, and establish an approximating Fokker-Planck-type equation (FPE) for  $p(t, \underline{\alpha})$ . The stochastic partial differential equations that generate this FPE according to the related well-established analogy<sup>[39]</sup> are then interpreted as the FHD model.

Zubarev and Morozov<sup>[38]</sup> work with long-wave Fourier components rather than with finite volume averages as their relevant observables, but their general approach can be transferred. For a system of  $N$ -particles of mass  $M$ , the observables used by Español<sup>[11]</sup> are, in contrast, the empirical mass, momentum, and energy

$$(\alpha_{ir}(t))_{i=1}^3 = \begin{pmatrix} m \\ mu \\ me \end{pmatrix}_r(t) = \sum_k^N \chi_r(\mathbf{x}_k(t)) \begin{pmatrix} M \\ M\dot{\mathbf{x}}_k(t) \\ M\dot{\mathbf{x}}_k(t)^2/2 + \phi_k(t) \end{pmatrix} \quad (25)$$

covered by the control volume  $r$  of a discrete grid or their densities

$$\alpha_r^* = \begin{pmatrix} \rho \\ \rho u \\ \rho e \end{pmatrix}_r = \frac{\alpha_r}{v_r} \quad (26)$$

Here,  $v_r$  is the volume of cell  $r$ ,  $\chi_r$  is its indicator function, and  $\phi_k$  is the total potential energy of the  $k$ th particle, induced through inter-particle interactions and external force fields. The empirical densities are also the relevant variables to be used in a finite volume computational fluid dynamics scheme in conservation form (see the next section).

Relying on arguments put forth by Zubarev and Morozov,<sup>[38]</sup> and assuming a large time scale separation between the dynamics of individual particles on the one hand and the empirical densities on the other, Español then derives a Fokker-Planck-type equation for the probability density of finding a CG state  $(\alpha_r)_{r \in R}$ , where  $R$  denotes the set of all grid cell indices. The derivation proceeds from (23), utilizing the definition of the probability density in the space of observables in (13). A lengthy calculation, not repeated here, yields the evolution equation of the observable space probability density  $p(\underline{\alpha}, t)$ ,

$$\partial_t p = -\partial_v \cdot (K_v p) + \partial_v \partial_\mu (D_{v\mu} p) \quad (27)$$

where we use the Einstein summation convention for the indices of the generalized vector of observables  $\underline{\alpha} = (\alpha_v)_{v \in \{1,2,3\} \times R}$ , let

$\partial_v \equiv \partial/\partial\alpha_v$ , and define

$$K_v(\underline{\alpha}) = v_v(\underline{\alpha}) + \frac{1}{Z(\underline{\alpha})} \partial_\mu (\zeta_{v\mu}(\underline{\alpha}) Z(\underline{\alpha})) \quad (28a)$$

$$v_v(\underline{\alpha}) = \langle \mathcal{L} A_v \rangle^\alpha \quad (28b)$$

$$\zeta_{v\mu}(\underline{\alpha}) = \int_0^\infty \langle (\mathcal{L} A_v - v_v(\underline{\alpha})) e^{s\mathcal{L}} (\mathcal{L} A_\mu - v_\mu(\underline{\alpha})) \rangle^\alpha ds \quad (28c)$$

$$D_{v\mu}(\underline{\alpha}) = \zeta_{v\mu}(\underline{\alpha}) + \zeta_{\mu v}(\underline{\alpha}) \quad (28d)$$

$$Z(\underline{\alpha}) = \int_\Omega \delta(\tilde{\underline{\mathbf{A}}}(\mathbf{X}) - \underline{\alpha}) f_0(\mathbf{X}) d\mathbf{X} \quad (28e)$$

Notice that the memory term in (23) collapses to a contribution to the second order diffusion-like term in (27) due to the time scale separation assumption, and that the effective diffusivity collects time correlations of fluctuations of the right hand side  $\mathcal{L}\tilde{\underline{\mathbf{A}}}$  of the observable evolution Equation (11) over the entire time horizon. Note also that the last term in Equation (23) cancels exactly from the evolution of the probability density.<sup>[33]</sup>

Equation (27) comes in the standard drift-diffusion form of a Fokker-Planck equation (FPE) for the observable-space probability density. Español,<sup>[11]</sup> building upon Español and Öttinger,<sup>[33]</sup> suggests to derive a FHD description from this equation using the well-known relationship between stochastic partial differential equations of Langevin type and FPEs. Along this route, and utilizing the transformation to densities from (26), Español derives the FHD equations

$$d\alpha_v^* = K_v^*(\underline{\alpha}^*) dt + B_{v\mu}(\underline{\alpha}^*) dW_\mu \quad (29)$$

where the  $dW_\mu$  denote a multi-component Wiener process with

$$dW_v(t) dW_\mu(t') = \begin{cases} \delta_{v\mu} dt & (t = t') \\ 0 & \text{otherwise} \end{cases} \quad (30)$$

while the drift term is

$$K_{ir}^*(\underline{\alpha}^*) = \frac{1}{v_r} K_{ir}(\underline{\alpha}) \quad (31)$$

and the multiplicative stochastic amplitude is the “square root” of the diffusion matrix from Equation (28) in the sense that

$$B_{ir,\mu'} B_{\mu',js}(\underline{\alpha}^*) = \frac{1}{v_r v_s} D_{ir,js}(\underline{\alpha}) \quad (32)$$

Of course,  $\alpha$  and  $\alpha^*$  are related through the definition of the densities in Equation (26) and we have again used Einsteins summation convention.

After these rather formal arguments, one may now ask what is the concrete explicit form of the FHD equation in Equation (29) and, in particular, whether there is any physical justification for the white noise forcing. In response, we refer first to Zubarev and Morozov<sup>[38]</sup> and Español<sup>[11]</sup> who explicitly demonstrate that for a “simple fluid,” and under the assumption of local equilibrium—velocity fluctuations are locally Gaussian with the identity as the

correlation matrix—and weak spatial variations that allow for Taylor expansions in gradients, the equations in (29) boil down to the explicit form of FHD referred to in subsequent sections,

$$\rho_i = -\nabla \cdot (\rho \mathbf{v}) \quad (33a)$$

$$(\rho \mathbf{v})_i = -\nabla \cdot (\rho \mathbf{v} \otimes \mathbf{v} + \sigma) \quad (33b)$$

$$(\rho e)_i = -\nabla \cdot (\mathbf{v}[\rho e] + \mathbf{v}\sigma + \mathbf{j}) \quad (33c)$$

where the fluxes  $\sigma, \mathbf{j}$  decompose into deterministic and fluctuating parts as

$$\sigma = p\mathbb{I} - 2\eta \left( \dot{\gamma} - \frac{1}{3} \text{tr}[\dot{\gamma}]\mathbb{I} \right) - \zeta \text{tr}[\dot{\gamma}]\mathbb{I} + \tilde{\sigma},$$

$$\dot{\gamma} = \frac{1}{2}[\nabla \mathbf{v} + (\nabla \mathbf{v})^T] \quad (34a)$$

$$\mathbf{j} = -\kappa \nabla T + \tilde{\mathbf{j}} \quad (34b)$$

Here,  $p$  is the local thermodynamic pressure,  $\mathbf{v}$  the flow velocity,  $\eta$  and  $\zeta$  are the dynamic shear and bulk viscosities, and  $\kappa$  is the heat conductivity. These quantities all satisfy the same formulae one obtains, for example, from the classical kinetic theory of gases.<sup>[14,40]</sup> The fluctuating momentum and heat fluxes,  $\tilde{\sigma}, \tilde{\mathbf{j}}$  are space-time decorrelated white noise perturbations, the detailed prescription of which in the more elaborate context of flows of multicomponent mixtures will be addressed in Section 2.3.7 below.

### 2.3.7. Compressible FHD Equations for Multicomponent Mixtures

To provide some insight into the current state of development of FHD models, we consider here the extension of FHD to nonideal mixtures, focusing on a compressible formulation. The generalization of FHD to binary mixtures was first presented by Cohen et al.<sup>[41]</sup> and by Law and Nieuwoudt.<sup>[42,43]</sup> The standard FHD theory for (thermo)diffusion in binary mixtures (see, for example, Ortiz de Zarate and Senger<sup>[44]</sup>) has recently been extended to nonideal ternary mixtures in thermodynamic equilibrium by Ortiz de Zarate et al.<sup>[45]</sup> Multicomponent gaseous systems are discussed within the GENERIC framework in the work of Öttinger.<sup>[46]</sup> Here we follow the development of the multicomponent ideal mixtures described in Balakrishnan et al.<sup>[47]</sup> extended to include nonideal effects as discussed in Donev et al.<sup>[48]</sup>

We consider a system with  $N_s$  species in the absence of any external forces. In this case, the species density, momentum, and energy equations of hydrodynamics are given by

$$\frac{\partial}{\partial t}(\rho_k) + \nabla \cdot (\rho_k \mathbf{v}) + \nabla \cdot \mathbf{F}_k = 0 \quad (35)$$

$$\frac{\partial}{\partial t}(\rho \mathbf{v}) + \nabla \cdot [\rho \mathbf{v} \mathbf{v}^T + p\mathbb{I}] + \nabla \cdot \boldsymbol{\tau} = 0 \quad (36)$$

$$\frac{\partial}{\partial t}(\rho E) + \nabla \cdot [(\rho E + p)\mathbf{v}] + \nabla \cdot [\mathbf{Q} + \boldsymbol{\tau} \cdot \mathbf{v}] = 0 \quad (37)$$

where  $\rho_k$ ,  $\mathbf{v}$ ,  $p$ , and  $E$  denote, respectively, the mass density for species  $k$ , fluid velocity, pressure, and total specific energy for the

mixture. Note that  $\mathbf{v}\mathbf{v}^T$  is a (tensor) outer product with  $T$  indicating transpose and  $\mathbb{I}$  is the identity tensor (i.e.,  $\nabla \cdot p\mathbb{I} = \nabla p$ ).

We note that mass conservation is exact, which requires that the species diffusion fluxes satisfies the constraint,

$$\sum_{k=1}^{N_s} \mathbf{F}_k = 0 \quad (38)$$

Summing the species equations then gives the continuity equation

$$\frac{\partial}{\partial t}\rho + \nabla \cdot (\rho \mathbf{v}) = 0 \quad (39)$$

where the total density  $\rho = \sum_{k=1}^{N_s} \rho_k$ .

To close the system we need to specify an equation of state and the transport terms. The equation of state specifies  $p = p(\rho, T, Y_k)$  where  $T$  is the temperature and  $Y_k = \rho_k/\rho$  are the mass fractions. The thermodynamic model of the system also species the internal energy  $e(\rho, T, Y_k)$ , which is related to the total energy by  $E = (e + \mathbf{v} \cdot \mathbf{v}/2)$ . The transport terms are given by the viscous tensor,  $\boldsymbol{\tau}$ , the species diffusion flux,  $\mathbf{F}$ , and heat flux,  $\mathbf{Q}$ . In FHD, we augment each of the transport fluxes in Equations (35)–(37) by adding a zero-mean stochastic flux to the deterministic flux. The covariance of these fluxes is chosen so that the equilibrium fluctuations match those specified by statistical mechanics. The Curie symmetry principle<sup>[49]</sup> says that fluxes and thermodynamics fluxes of different tensorial character do not couple so we can consider viscosity separately from species and thermal diffusion. In each case, we need to specify the deterministic flux and the stochastic flux.

For Newtonian fluids, the deterministic viscous tensor is

$$\bar{\boldsymbol{\tau}} = -\eta(\nabla \mathbf{v} + (\nabla \mathbf{v})^T) - \left( \kappa - \frac{2}{3}\eta \right) \mathbb{I}(\nabla \cdot \mathbf{v}) \quad (40)$$

where  $\eta$  and  $\kappa$  are the shear and bulk viscosity, respectively. We now want to augment the deterministic stress tensor with a stochastic flux  $\boldsymbol{\tau} = \bar{\boldsymbol{\tau}} + \tilde{\boldsymbol{\tau}}$  where  $\langle \tilde{\boldsymbol{\tau}} \rangle = 0$  with  $\langle \rangle$  denoting a suitably defined ensemble average. The stochastic viscous flux tensor is a Gaussian random field that can be written as<sup>[11,50]</sup>

$$\tilde{\boldsymbol{\tau}}(\mathbf{r}, t) = \sqrt{2k_B T \eta} \tilde{\mathcal{Z}}^v + \left( \sqrt{\frac{k_B \kappa T}{3}} - \sqrt{\frac{2k_B \eta T}{3}} \right) \text{Tr}(\tilde{\mathcal{Z}}^v) \quad (41)$$

where  $k_B$  is Boltzmann's constant,  $T$  is temperature and  $\tilde{\mathcal{Z}}^v = (\mathcal{Z}^v + (\mathcal{Z}^v)^T)/\sqrt{2}$  is a symmetric Gaussian random tensor field. (The  $\sqrt{2}$  in the denominator accounts for the variance reduction from averaging.) Here  $\mathcal{Z}^v$  is a white-noise random Gaussian tensor field; i.e.,

$$\langle \mathcal{Z}_{\alpha\beta}^v(\mathbf{r}, t) \mathcal{Z}_{\gamma\delta}^v(\mathbf{r}', t') \rangle = \delta_{\alpha\gamma} \delta_{\beta\delta} \delta(\mathbf{r} - \mathbf{r}') \delta(t - t')$$

Next, we need to formulate the species diffusion and heat fluxes. As with the viscosity, we require both a deterministic and a stochastic flux. In this case, the construction is complicated by cross-diffusion of species and thermal diffusion effects (Soret and Dufour). The formulation of the fluxes is based on the entropy production for a mixture, as formulated by de Groot and

Mazur<sup>[49]</sup> and by Kuiken.<sup>[51]</sup> Entropy production establishes the deterministic form of the thermodynamics forces and fluxes. The fluctuation dissipation principle is then used to specify the noise.

The entropy production arising from gradients in species concentration and temperature are given by

$$\mathbf{v} = -\frac{1}{T^2} \mathbf{Q}' \cdot \nabla T - \frac{1}{T} \mathbf{F}^T \cdot \nabla_T \mu \quad (42)$$

where  $\mu$  is the vector of chemical potentials per unit mass of each species,  $\mathbf{F}$  is the vector of species fluxes and the reduced heat flux is given by

$$\mathbf{Q}' = \mathbf{Q} - h^T \mathbf{F} \quad (43)$$

where  $h$  is the vector of specific enthalpies. (When required we denote components of a vector with a subscript; i.e.,  $h_k$  is the  $k^{\text{th}}$  component of  $h$ .) In other words,  $\mathbf{Q}'$  is the part of the heat flux that is not associated with mass diffusion.

For the discussion here, we assume the chemical potentials to be functions of  $p$ ,  $T$  and the mole fractions,  $X$ , where  $X_k = n_k / \sum_{j=1}^{N_s} n_j$  with number densities,  $n_k$ . Here,  $\nabla_T$  is a gradient taken holding temperature fixed, that is,

$$\nabla_T \mu_k(p, T, X) = \nabla \mu_k - \left( \frac{\partial \mu_k}{\partial T} \right)_{p, X} \nabla T \quad (44)$$

The mole fractions can also be written in terms of the mass fractions as

$$X = \bar{m} \mathcal{M}^{-1} Y \quad (45)$$

where  $\mathcal{M}$  is a diagonal matrix of molecular masses and  $\bar{m} = (\sum_{k=1}^{N_s} Y_k / m_k)^{-1}$  is the mixture-averaged molecular mass.<sup>[51]</sup>

The general form of the phenomenological laws expresses the fluxes as linear combinations of thermodynamic forces<sup>[49]</sup>

$$\mathbf{J} = \mathbf{L} \mathbf{X} \quad (46)$$

where the fluxes  $\mathbf{J}$  and thermodynamic forces  $\mathbf{X}$  are given by

$$\mathbf{J} = \begin{bmatrix} \mathbf{F} \\ \mathbf{Q}' \end{bmatrix} \quad \text{and} \quad \mathbf{X} = \begin{bmatrix} -\frac{1}{T} \nabla_T \mu \\ \frac{\nabla T}{T^2} \end{bmatrix} \quad (47)$$

Onsager reciprocity say that the matrix  $\mathbf{L}$  is symmetric; hence, it can be written in the form

$$\mathbf{L} = \begin{bmatrix} \mathbf{L} & \mathbf{l} \\ \mathbf{l}^T & \ell \end{bmatrix} \quad (48)$$

Here,  $\mathbf{L}$  is a positive semi-definite matrix whose rank is one less than the number of species in the system, reflecting the constraint that mole (and mass) fractions sum to 1.

Before constructing the noise for the system, we note that we can write the Onsager matrix  $\mathbf{L}$  in a modified form by defining  $\xi$  such that  $\mathbf{l} = \mathbf{L} \xi$ . This construction is feasible because  $\mathbf{l}$  is in the range of  $\mathbf{L}$ . Note that  $\xi$  is not uniquely determined. We choose  $\xi$  such that  $\xi^T \mathbf{u} = 0$  where  $\mathbf{u}$  is a vector of all ones. We also define

$\zeta = \ell - \xi^T \mathbf{L} \xi$ . With these definitions, the Onsager matrix can be written as

$$\mathbf{L} = \begin{bmatrix} \mathbf{L} & \mathbf{L} \xi \\ \xi^T \mathbf{L} & \zeta + \xi^T \mathbf{L} \xi \end{bmatrix} \quad (49)$$

Öttinger<sup>[46]</sup> gives a derivation of this form using the GENERIC formalism subject to the linear constraint  $\sum_{k=1}^{N_s} Y_k = 1$ . From Equation (49) we can then obtain the deterministic species flux

$$\mathbf{F} = -\frac{1}{T} \mathbf{L} \left[ \nabla_T \mu + \frac{\xi}{T} \nabla T \right] \quad (50)$$

and the deterministic heat flux

$$\mathbf{Q} = -\zeta \frac{\nabla T}{T^2} + (\xi^T + \mathbf{h}^T) \mathbf{F} \quad (51)$$

We now want to establish the form of the stochastic fluxes in the FHD equations. Since these fluxes are white in space and time we can write them in the form

$$\tilde{\mathbf{J}}_\alpha = \mathcal{B} \mathcal{Z}^{(\alpha)} \quad \text{where} \quad \tilde{\mathbf{J}}_\alpha = \begin{bmatrix} \tilde{\mathbf{F}}_\alpha \\ \tilde{\mathbf{Q}}_\alpha \end{bmatrix} \quad \text{and} \quad \mathcal{Z}^{(\alpha)} = \begin{bmatrix} \mathcal{Z}^{(F;\alpha)} \\ \mathcal{Z}^{(Q';\alpha)} \end{bmatrix} \quad (52)$$

where  $\alpha = x, y, z$  denotes spatial direction and  $\mathcal{Z}^{(F;\alpha)} = [\mathcal{Z}^{(1;\alpha)}, \dots, \mathcal{Z}^{(N_s;\alpha)}]^T$  is a vector of independent Gaussian white noise terms, that is,

$$\langle \mathcal{Z}^{(i;\alpha)}(\mathbf{r}, t), \mathcal{Z}^{(j;\beta)}(\mathbf{r}', t') \rangle = \delta_{ij} \delta_{\alpha\beta} \delta(\mathbf{r} - \mathbf{r}') \delta(t - t'),$$

$$\langle \mathcal{Z}^{(Q';\alpha)}(\mathbf{r}, t), \mathcal{Z}^{(Q';\beta)}(\mathbf{r}', t') \rangle = \delta_{\alpha\beta} \delta(\mathbf{r} - \mathbf{r}') \delta(t - t')$$

and  $\langle \mathcal{Z}^{(F;\alpha)} \mathcal{Z}^{(Q';\beta)} \rangle = 0$ .

To satisfy fluctuation dissipation balance, we need<sup>[44,45]</sup>

$$\mathcal{B} \mathcal{B}^T = 2k_B \mathbf{L} \quad (53)$$

Thus  $\mathcal{B}$  represents a scaled square root of  $\mathbf{L}$ . The form of  $\mathcal{B}$  is not unique; however, if we introduce the Cholesky factorization  $\mathbf{B}$  of  $\mathbf{L}$ ; that is,  $\mathbf{L} = \mathbf{B} \mathbf{B}^T$  and define

$$\mathcal{B} = \sqrt{2k_B} \begin{bmatrix} \mathbf{B} & \mathbf{0} \\ \xi^T \mathbf{B} & \sqrt{\zeta} \end{bmatrix} \quad (54)$$

then the resulting matrix satisfies Equation (53).

The species diffusion noise is then given by  $\tilde{\mathbf{F}}_\alpha = \mathbf{B} \mathcal{Z}^{(F;\alpha)}$  and the augmented stochastic heat flux is thus given by

$$\tilde{\mathbf{Q}}_\alpha = \sqrt{\zeta} \mathcal{Z}^{(Q';\alpha)} + (\xi^T + \mathbf{h}^T) \tilde{\mathbf{F}}_\alpha$$

We note that although  $\mathbf{B}$  is of size  $N_s \times N_s$ , only  $N_s - 1$  noise terms are needed because the last column of  $\mathbf{B}$  is identically zero, reflecting the singularity of  $\mathbf{L}$ .

The discussion above presents the species diffusion and heat flux in the form used in nonequilibrium thermodynamics.<sup>[49]</sup> We now want to recast both the deterministic and stochastic diffusive fluxes in the Fickian form more typically used in the transport literature. See Giovangigli<sup>[52]</sup> for additional details of this construction and how the Fickian diffusion matrix is computed



from Maxwell–Stefan binary diffusion coefficients. In the Fickian description, the diffusion is expressed in terms of gradients of  $X$  and  $p$  rather than in terms of gradients of chemical potential,  $\mu$ . This is not simply a cosmetic difference. The gradient of the chemical potential for a given species has a singularity when that species vanishes. In the Onsager form of diffusion  $\mathbf{L}$  vanishes when a species vanishes, which cancels the singularity. In the Fickian form, this singularity is canceled analytically.

Here, we include nonideal effects so that we can model transport in liquids. At a fundamental level, these nonideal effects are expressed in terms of the Gibbs free energy,  $g$ . The chemical potentials per unit mass are given by

$$\mu(X, T, p) = \frac{\partial g}{\partial Y} \quad (55)$$

Each chemical potential can then be decomposed into an ideal contribution and an excess contribution to give

$$\mu(X, T, p) = \mu^{(id)} + \mu^{(ex)} = (\mu^0(T, p) + k_B T \mathcal{M}^{-1} \ln(X)) + \mu^{(ex)} \quad (56)$$

From this definition, we can define the matrix of thermodynamic factors

$$\Gamma = \frac{\bar{m}}{k_B T} \mathcal{Y} \frac{\partial \mu}{\partial X} = I + \frac{\bar{m}}{k_B T} \mathcal{Y} \frac{\partial \mu^{(ex)}}{\partial X} \quad (57)$$

where  $\mathcal{Y}$  is the diagonal matrix of mass fractions. In the engineering literature<sup>[51]</sup> the excess chemical potential is often described in terms of the logarithm of an activity coefficient. The second term on the right hand side of (57) represents the derivative of the activity coefficients with respect to composition. However, recalling that  $\mu^{(ex)} = \partial g^{(ex)} / \partial Y$  we have that

$$\begin{aligned} \Gamma &= I + \frac{\bar{m}}{k_B T} \mathcal{Y} \frac{\partial}{\partial X} \frac{\partial g^{(ex)}}{\partial Y} = I + \frac{\bar{m}}{k_B T} (\mathcal{X} - \mathbf{X}\mathbf{X}^T) \frac{\partial^2 g^{(ex)}}{\partial X^2} \\ &= I + (\mathcal{X} - \mathbf{X}\mathbf{X}^T) H \end{aligned} \quad (58)$$

where  $\mathcal{X}$  is the diagonal matrix of mole fractions and

$$H = \frac{\bar{m}}{k_B T} \frac{\partial^2 g^{(ex)}}{\partial X^2} \quad (59)$$

is the Hessian of the excess free energy per particle. This form shows the linkage between nonideal transport effects and the Gibbs free energy and provides a more fundamental characterization that is directly linked to thermodynamic stability.<sup>[48]</sup>

With these definitions, we can now compute

$$\nabla_T \mu = \frac{\partial \mu}{\partial X} \nabla X + \frac{\partial \mu}{\partial p} \nabla p \quad (60)$$

$$= \frac{k_B T}{\bar{m}} \mathcal{Y}^{-1} \left[ \Gamma \nabla X + \frac{\bar{m}}{k_B T} \mathcal{Y} \theta \nabla p \right] \quad (61)$$

$$= \frac{k_B T}{\bar{m}} \mathcal{Y}^{-1} \left[ \Gamma \nabla X + \frac{\bar{m}}{k_B \rho T} \phi \nabla p \right] \quad (62)$$

where  $\theta = \partial \mu / \partial p$  and  $\phi = \rho \mathcal{Y} \theta$ .

We then define the diffusion driving force as

$$d = \frac{k_B T}{\bar{m}} \left[ \Gamma \nabla X + \frac{\bar{m}}{k_B \rho T} (\phi - Y) \nabla p \right] \quad (63)$$

This is the quantity inside the braces in Equation (62) minus

$$\frac{\bar{m}}{k_B \rho T} Y \nabla p \quad (64)$$

This additional term is added to normalize the diffusion driving forces so that they sum to zero.

The deterministic species fluxes can now be expressed in Fickian form as

$$\bar{\mathbf{F}} = \rho \mathcal{Y} D \left[ d + \frac{\chi}{T} \nabla T \right] \quad (65)$$

where  $\chi$  is the vector of thermal diffusion ratios. As noted above, the matrix of diffusion coefficients,  $D$ , can be computed from binary diffusion using the Maxwell–Stefan description of diffusion; see refs. [48, 52].

Comparing with the Onsager form we then have

$$\mathbf{L} = \frac{\bar{m} \rho}{k_B} \mathcal{Y} D \mathcal{Y} \quad \text{and} \quad \xi = \frac{k_B T}{\bar{m}} \mathcal{Y}^{-1} \chi \quad \text{and} \quad \zeta = T^2 \lambda \quad (66)$$

Using these relationships we can now compute both deterministic and stochastic species diffusion and heat flux from standard transport properties.

### 2.3.8. Chemical Reactions

The multicomponent FHD framework discussed can be extended to include chemical reactions. Unlike the transport processes, chemistry cannot be viewed in the framework of linearized phenomenological Onsager theory. Except in rare circumstances, chemical reactions are typically not sufficiently close to equilibrium. However, it is still possible to derive a stochastic representation of chemical reactions from the chemical master equation.<sup>[53]</sup> The resulting equation, referred to as the chemical Langevin equation can then be coupled to FHD.<sup>[54]</sup>

When there are a sufficiently large number of reactants, the chemical Langevin equation provides an accurate model of chemical processes. However, when the number of reactants becomes small, the approximation breaks down and an alternative approach is required. For small numbers of reactants an approximation based on Poisson statistics that more closely approximates the chemical master equation is needed. One candidate for a model for reactions in the small reactant limit is the stochastic simulation algorithm (SSA) of Gillespie<sup>[55]</sup> that directly samples the chemical master equation using an event driven approach. A more efficient variant of SSA is the tau-leaping approach first introduced by Gillespie<sup>[56]</sup> that approximates the master equation by estimating the number of reactions within a time step using Poisson random numbers. The tau-leaping approach has been coupled to an FHD-based model of diffusion<sup>[57]</sup> and to a low Mach number hydrodynamics algorithm.<sup>[58]</sup>

## 2.4. Summary of and Conclusions from Section 2

Grid-based FHD models have matured over the past two decades to become versatile tools for the study of non-equilibrium effects in inert and reacting fluids on meso-scales, that is, on scales in between those accessible by molecular dynamics on the one hand and deterministic continuum mechanics on the other hand. FHD models have successfully been coupled to particle-based fluid representations in various contexts, but these efforts thus far involved predominantly CG molecular models or direct particle-based discretizations of continuum mechanics. In contrast, the construction of such hybrid models with atomistic MD at the particle end of the coupling interface has gained momentum only rather recently. In the authors' view, the following issues and considerations deserve attention in this context:

**Advantages of Conservative Finite Volume Discretizations of FHD:** Model equations for FHD have been formulated in terms of various spatial representations. The pioneering work by Zubarev and Morozhov<sup>[38]</sup> utilized the long-wave Fourier modes of the field variables as the relevant FHD variables. Español<sup>[11]</sup> suggested finite volume balances of mass, momentum, and energy, while more recently Español et al.<sup>[59,60]</sup> introduced a formulation akin to unstructured grid finite element schemes for computational fluid dynamics. In the present discussion of particle-continuum hybrid models, the focus is on finite volume methods for FHD for the following reasons: The hybrid models considered here employ atomistic MD on finite subdomains of the flow field, and information exchange between the MD and FHD subdomains is naturally organized via fluxes of mass, momentum, and energy. The embedding of such a model in a finite volume-based FHD solver naturally fits the discrete structure of the discretized continuum model in this sense.

**Validity of Time Scale Separation Assumption and Markovianity:** Most FHD implementations do not account for non-Markovian (memory) effects. The only exception the authors are aware of is work of Voulgarikas et al.<sup>[61]</sup> who extend FHD to non-Markovian rheological models and colored noise. Utilizing standard existing models therefore implies a sufficient level of coarse-graining or, in turn, a sufficiently large particle numbers in the coupled MD subdomain to justify this assumption. An interesting future research question then concerns the quantification of these limitations: Thus, according to Bian et al.,<sup>[62]</sup> particle numbers of a few hundred molecules in the MD part of a hybrid model—a number that has been repeatedly used with success in studies of equilibrium situations, see e.g. Jabes et al.<sup>[63]</sup>—suffice in this sense. If higher quantitative accuracy is needed, are there efficient extensions of finite volume FHD that account for the finite size effects in time correlation functions observed by these authors, or for memory effects?

**Long Wave Information and Hybrid Modeling:** Long-range correlations in non-equilibrium systems can induce “giant fluctuations” on scales far beyond the atomistic ones.<sup>[47,48,64]</sup> Successful representation of the net effects of such fluctuations evidently requires computational domains that cover at least a few multiples of the giant fluctuations' scales. As a consequence, hybrid modelling becomes even a necessity when non-equilibrium dynamics is to be represented by atomistic MD on limited subdomains.

## 3. Molecular Dynamics (MD) and (Particle-Based) Multiscale Simulations

Atomistic MD simulations provide us with a wealth information about the structural and dynamic properties of complex molecular systems at the atomistic length scales including hydrodynamic effects if an explicit solvent is included in our molecular model.<sup>[65,66]</sup> In MD simulations,<sup>[66]</sup> the time evolution of a system is computed employing the classical Newton equations of motion:

$$\frac{d\mathbf{r}_i}{dt} = \mathbf{v}_i \quad (67)$$

$$m_i \frac{d\mathbf{v}_i}{dt} = \mathbf{F}_i \quad (68)$$

where  $\mathbf{r}_i$ ,  $\mathbf{v}_i$ ,  $\mathbf{F}_i$  are the position, velocity, and forces acting on the  $i$ th particle with mass  $m_i$ . Statistical properties of the system are computed as time averages over the trajectories. If we assume that the system is ergodic<sup>[67]</sup> then the time-averaged statistical properties match the ones computed from the corresponding microcanonical statistical ensemble in the thermodynamic limit.<sup>[65]</sup> However, due to the computational complexity related to studying, for example, biomolecular systems, MD simulations still have limitations in reaching experimentally required time and length scales. In particular, simulating a solvent explicitly is computationally the most expensive part in all-atom biomolecular simulations because of a huge number of corresponding degrees of freedom.<sup>[68]</sup> The computational burden is drastically alleviated by implicit solvent models but if one is interested in hydrodynamic interactions the inclusion of explicit solvent is in many cases unavoidable.<sup>[69,70]</sup>

Coarse-graining approaches, of which some basic aspects have already been introduced in the previous sections, drastically reduce the number of degrees of freedom in the system and became rather popular for the simulation of molecular systems at the mesoscale level.<sup>[71–73]</sup> In particular, in chemical physics and biophysics applications, coarse-graining can be done both in a bottom-up fashion,<sup>[74–82]</sup> in that one builds a given CG solvent model based on an underlying atomistic model and/or in a top-down way,<sup>[83–90]</sup> as for example, in the DPD method.<sup>[24,91–97]</sup> Typically, the atomistic resolution is mandatory only in the first few hydration layers around solvated biomolecules to properly account for the interaction between water and the biomolecules. The rest of the system then plays merely the role of a thermodynamic bath. The most efficient way to tackle such situations is using multiscale modeling approaches, in particular, concurrent multiscale methods, which couple fine- and CG resolutions at the same time in the simulation box, for example, refs. [6, 7, 98–117].

Some of us have been developing a particularly efficient scheme of concurrent coupling in the course of the years that is called the Adaptive Resolution Scheme (AdResS).<sup>[18,118,119]</sup> In such a scheme, molecules can change their resolution on-the-fly during the course of an MD simulation according to the region where they are instantaneously located. This scheme, allowing for the dynamic exchange of particles between different regions at different resolution, is an optimal basis for the coupling with the hydrodynamic scale. In fact, from the point of view of fluid

dynamics, the hydrodynamic/macroscale is typically connected to the atomistic scale by calculating local continuum mechanical properties in attached atomistic MD simulations with fixed relatively small particle numbers. The mean statistical properties of these local MD simulations are synchronized after every few time steps to the local fluid state to maintain consistency with the continuum mechanical equations (see e.g., refs. [120, 121]). On the one hand, it is clear that the fixed number of particles in any fluid element is a nonphysical hypothesis which of course imposes a bias on, for example, local particle density fluctuations. On the other hand, from the point of view of atomistic simulations, it is typically assumed that beyond the region of chemical interest, with fixed number of molecules, the system can be sufficiently described as a generic, large scale, electrostatic continuum (see e.g., ref. [122]). Obviously also in this case there is

forces are computed from the AT ( $U^{AT}$ ) and CG ( $U^{CG}$ ) potentials as

$$\mathbf{F}_{\alpha\beta}^{AT} = - \sum_{i\alpha,j\beta} \frac{\partial U^{AT}}{\partial \mathbf{r}_{i\alpha j\beta}} \quad \text{and} \quad \mathbf{F}_{\alpha\beta}^{CG} = - \frac{\partial U^{CG}}{\partial \mathbf{r}_{\alpha\beta}} \quad (71)$$

The sum runs over of all pair atom interactions between explicit atoms  $i$  of the molecule  $\alpha$  and explicit atoms  $j$  of the molecule  $\beta$ . The vector  $\mathbf{r}_{\alpha\beta} = \mathbf{r}_{\alpha} - \mathbf{r}_{\beta}$  connects the centers of mass (CoM) of molecules  $\alpha$  and  $\beta$ , while  $\mathbf{r}_{i\alpha j\beta} = \mathbf{r}_{i\alpha} - \mathbf{r}_{j\beta}$  is the relative position vector of atoms  $i$  and  $j$ . A smooth transition from the AT to CG representations and vice-versa is enabled with the hybrid (HY) region ( $R_{AT} < R < R_{CG}$ ). Two different interpolations of forces have been proposed: the original<sup>[118]</sup> and the “reverse” definition.<sup>[124]</sup> The  $\lambda$  is respectively given by

$$\lambda(\mathbf{r}_{\alpha}, \mathbf{r}_{\beta}) = \begin{cases} w(\mathbf{r}_{\alpha})w(\mathbf{r}_{\beta}); & w(\mathbf{r}_{\alpha\beta}) = \begin{cases} 1, & \text{AT} \\ \cos^2 \left[ \frac{\pi(\|\mathbf{r}_{\alpha\beta} - \mathbf{r}_0\| - R_{AT})}{2(R_{CG} - R_{AT})} \right], & \text{HY} \\ 0, & \text{CG} \end{cases} \\ 1 - w(\mathbf{r}_{\alpha})w(\mathbf{r}_{\beta}); & w(\mathbf{r}_{\alpha\beta}) = \begin{cases} 0, & \text{AT} \\ \cos^2 \left[ \frac{\pi(R_{CG} - \|\mathbf{r}_{\alpha\beta} - \mathbf{r}_0\|)}{2(R_{CG} - R_{AT})} \right], & \text{HY} \\ 1, & \text{CG} \end{cases} \end{cases}; \quad \begin{matrix} \text{original} \\ \text{reverse} \end{matrix} \quad (72)$$

a bias on local particle density fluctuations. The adaptive resolution technique instead can automatically satisfy both points of view by allowing the natural exchange of particles consistently with microscopic and macroscopic equations. For this reason, in this paper the adaptive resolution scheme is taken as a prototype for coupling the scales, but of course we must underline that it does not necessarily represent the unique path to coupling, this point will be underlined later by providing references of similar and complementary couplings.

### 3.1. Adaptive Resolution Scheme(AdResS)

Resorting to AdResS,<sup>[18,119]</sup> the total force acting on a molecule  $\alpha$  is

$$\mathbf{F}_{\alpha} = \mathbf{F}_{\alpha}^{AdResS} + \mathbf{F}_{\alpha}^{TD} + \mathbf{F}_{\alpha}^{thermo} \quad (69)$$

where  $\mathbf{F}_{\alpha}^{AdResS}$  is the force coupling atomistic and CG descriptions,  $\mathbf{F}_{\alpha}^{TD}$  is the thermodynamic force, and  $\mathbf{F}_{\alpha}^{thermo}$  is the thermostat contribution. The AdResS force, which is, in general, non-conservative, is defined as

$$\mathbf{F}_{\alpha}^{AdResS} = \sum_{\beta \neq \alpha} \left\{ \lambda(\mathbf{r}_{\alpha}, \mathbf{r}_{\beta}) \mathbf{F}_{\alpha\beta}^{AT} + [1 - \lambda(\mathbf{r}_{\alpha}, \mathbf{r}_{\beta})] \mathbf{F}_{\alpha\beta}^{CG} \right\} \quad (70)$$

where  $\mathbf{F}_{\alpha\beta}^{AT}$  and  $\mathbf{F}_{\alpha\beta}^{CG}$  are atomistic (AT) and CG forces, respectively, between molecules  $\alpha$  and  $\beta$  (see also **Figure 1**, panel (a)). The

In both implementations, the weighting function  $w$  is a smooth sigmoid function with extreme values of 0 and 1. However, it is defined for the computational benefits upside down in the “reverse” implementation. In Equation (72),  $\mathbf{r}_0$  denotes the center of the AT region, which can be either a fixed point (usually the center of the simulation box) or a mobile point, as for example, in a simulation of a protein where it coincides with the protein’s CoM. AdResS can accommodate various geometric boundaries between the resolution regions: splitting in 1 dimension,<sup>[125]</sup> cylindrical,<sup>[126]</sup> spherical.<sup>[127]</sup> It also permits the use of flexible domains<sup>[128]</sup> where the atomistic region is defined as a distance from the surface of the macromolecule which is beneficial for multiscale simulations of macromolecules that change their shape during the simulation, for example, proteins that fold or unfold.

The thermodynamic force  $\mathbf{F}^{TD}$  accommodates the coupling of rather loosely connected molecular representations, that is, it maintains two different models with, in general, different thermodynamic properties like pressure and chemical potential in thermodynamic equilibrium.<sup>[129–131]</sup> Typically, there is a preferential tendency of the molecules to migrate into the low-resolution domain with lower chemical potential density. This effect is manifested as density undulations across the direction of the resolution change. The thermodynamic force, which corrects for these undulations, is defined as the negative derivative of the chemical potential density, and is numerically computed iteratively as

$$\mathbf{F}_{k+1}^{TD}(\|\mathbf{r} - \mathbf{r}_0\|) = \mathbf{F}_k^{TD} - C \nabla \rho_k(\|\mathbf{r} - \mathbf{r}_0\|) \quad (73)$$

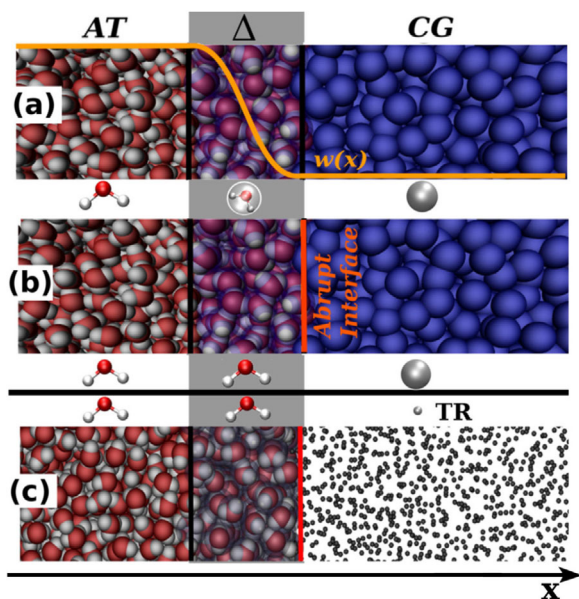


**Figure 1.** a) Schematic representation of the original version of AdResS. AT indicates the region at atomistic resolution,  $\Delta$  (HY), represents the transition region where molecules have hybrid atomistic/coarse-grained resolution, regulated by the switching function  $w(x)$ , finally, CG is the region at coarse-grained resolution. b) Schematic representation of a most recent version of AdResS: the change of resolution is no more regulated by  $w(x)$  in  $\Delta$ . Atomistic and coarse-grained molecules are directly coupled. The  $\Delta$  region is now chosen large enough to allow molecules to equilibrate upon entering the AT region. c) Schematic representation of an extension of the version above, relevant for this paper. The CG region is reservoir of non-interacting point-like particles brought into equilibrium through the action of the  $\Delta$  region and of a thermostat. In addition, the thermodynamic force is calculated and applied over the whole  $\Delta \cup \text{TR}$  region. Reproduced under the terms of the CC-BY-NC license.<sup>[123]</sup> Copyright 2019, The Authors. Published by Wiley-VCH.

Here  $k$  denotes the iteration step and  $C = \frac{M}{\rho_0^2 \kappa_T}$ , with  $\rho_0$  and  $\kappa_T$  the bulk density and isothermal compressibility. The iteration based on Equation (73) is terminated after, say, the  $n$ th step if the density reaches a certain accuracy in matching the target density in the  $\Delta$  region. The criterion used is  $\max_{\Delta} |\rho_0 - \rho_n| \leq \epsilon$ , where an extended experience with applications has shown that  $\epsilon \leq 0.03$  yields satisfactory accuracy. In most of the applications, however,  $\epsilon$  is chosen below 0.01. It was also empirically found that in practice  $C$  can be adjusted along the process to prevent under/over correction and to speed up the iteration procedure without producing artifacts in the simulation results. Thus, in practice, we run several simulations with different prefactors simultaneously at each iteration step and select the best one for the next iteration. Admittedly, we have thus far not found a systematic procedure with provable convergence, so that this aspect remains as an interesting challenge for future research.

Note that the force definition in Equation (70) satisfies Newton's third law, that is,  $F_{\alpha\beta} = -F_{\beta\alpha}$ . However, since the total pair force depends not only on their relative distances but also on the absolute positions of the molecules, it is not conservative and the corresponding potential does not exist. This implies the use of a local thermostat that supplies or removes the latent heat caused by the switch of resolution.<sup>[118]</sup> Since we are interested in a proper

description of hydrodynamics interactions, we focus here on a local thermostat that preserves the linear momentum, that is, the DPD<sup>[132,133]</sup>:

$$\begin{aligned} F_{\alpha}^{\text{thermo}} &= F_{\alpha}^D + F_{\alpha}^R \\ F_{\alpha}^D &= \sum_{\beta \neq \alpha} F_{\alpha\beta}^D & F_{\alpha\beta}^D &= -\gamma \omega^D(R_{\alpha\beta}) (\hat{\mathbf{r}}_{\alpha\beta} \mathbf{v}_{\alpha\beta}) \hat{\mathbf{r}}_{\alpha\beta} \\ F_{\alpha}^R &= \sum_{\beta \neq \alpha} F_{\alpha\beta}^R & F_{\alpha\beta}^R &= \sqrt{2\gamma k_B T} \omega^R(R_{\alpha\beta}) \eta_{\alpha\beta} \hat{\mathbf{r}}_{\alpha\beta} \end{aligned} \quad (74)$$

where  $\mathbf{v}_{\alpha\beta} = \mathbf{v}_{\alpha} - \mathbf{v}_{\beta}$  is the velocity between the clusters individual particles that are grouped into the effective DPD particles  $\alpha$  and  $\beta$ . The noise  $\eta_{\alpha\beta}$  must satisfy  $\langle \eta_{\alpha\beta} \rangle = 0$  and  $\langle \eta_{\alpha\beta}(t) \eta_{\alpha'\beta'}(t') \rangle = 2(\delta_{ik} \delta_{jl} + \delta_{il} \delta_{kj}) \delta(t - t')$ . The  $\omega^D(R_{\alpha\beta})$  and  $\omega^R(R_{\alpha\beta})$  are  $R$ -dependent weight functions that vanish at a predefined cut-off radius. From the fluctuation–dissipation theorem it follows that  $(\omega^R(R_{\alpha\beta}))^2 = \omega^D(R_{\alpha\beta})$ . Equation (74) is written only for the CG region, as they are analogous for the AT domain. Instead of a CG particle representing only a single solvent molecule, AdResS can be also used to couple atomistic liquid models with supramolecular models such as MARTINI and DPD, where several water molecules are represented with a single CG bead. To this end, we have developed a dynamic clustering algorithm SWINGER that can concurrently assemble, disassemble, and reassemble water bundles, consisting of several water molecules.<sup>[69,124,125,134]</sup> Thus, it allows for a seamless coupling between standard atomistic and supramolecular water models in adaptive resolution simulations. Our multiscale approach paves the way for efficient multiscale simulations of biomolecular systems without compromising the accuracy of atomistic water models. This is essential for future nanofluidics and nanomedical applications.<sup>[109,135–137]</sup>

### 3.2. Specific Examples of Adaptive Resolution for MD/Continuum Coupling

The adaptive resolution technique naturally stimulates the idea of extending the resolution interface beyond particle-based methods to the continuum. Here, we report a few recent hybrid approaches toward technically interfacing MD and mesoscopic hydrodynamics, which are either based on or adapt a similar coupling strategy as AdResS. In the approach of Petsev et al.,<sup>[111,138–140]</sup> AdResS is used to couple MD to smoothed dissipative particle dynamics (SDPD).<sup>[141]</sup> SDPD is a particle-based, Lagrangian, continuum solver used to numerically, in an MD-like fashion, solve Navier–Stokes equations. SDPD is a fluctuating extension of smoothed particle hydrodynamics (SPH),<sup>[142,143]</sup> incorporating thermal fluctuations. On the other hand, Alkseeva et al.<sup>[144]</sup> applied AdResS to link MD with multiparticle collision dynamics (MPC).<sup>[145]</sup> MPC is a mesoscale simulation method for fluid flows, where the fluid is modeled by particles with continuous positions and velocities and stochastic interparticle interactions. The fluid is discretized into cells with no restriction on the number of particles in each cell.<sup>[145]</sup> MPC models hydrodynamics on large length and times scales and locally conserves mass, momentum, and energy. Another hybrid method has been presented in refs. [113, 146–148]. A hybrid MD/continuum setup



was introduced where the two fluid descriptions were considered as two completely miscible liquids, that is, one phase corresponding to the MD and the other to FHD. Coupling between the two models is carried out by allowing exchange of mass and momentum between the two phases and introducing an order parameter playing a similar role as the weighting function in AdResS that quantifies the distribution of mass and momentum between the MD and continuum phases.

### 3.3. Coupling MD with Computational Fluid Dynamics (CFD)

Concurrent coupling strategies that aim to couple atomistic and continuum descriptions of liquids need to ensure that physical quantities, for example, density, momentum, energy, and the corresponding fluxes, are continuous across the interface between the two regimes where atomistic and continuum domains provide each other with boundary conditions. To impose boundary conditions from the atomistic to continuum domain is rather straightforward since it essentially deals with standard temporal and spatial averaging. But imposing the continuum boundary conditions on the particle domain presents the major methodological issue to be dealt with. To that end, there have been two kinds of schemes reported in the literature: methods that employ the state-variable coupling<sup>[107,109,149–153]</sup> and methods based on flux-exchange.<sup>[6,154–157]</sup> The latter are especially convenient for coupling MD to FHD.<sup>[155,158,159]</sup> For example, one can also couple FHD directly to a single particle (a colloid) using a hybrid Eulerian–Lagrangian approach.<sup>[60,160–163]</sup> Another example of methods that treat solvent using a continuum approach and solutes as particles is a hybrid method,<sup>[164]</sup> which couples MD with the Lattice–Boltzmann method (LBM).<sup>[165]</sup> This hybrid approach enables simulations of polymer–solvent systems, where the solvent is modeled by LBM and polymers by MD. Furthermore, a CFD solver can also be employed in the total simulation domain and the MD is only used to provide fine details such as boundary conditions or constitutive relations wherever required.<sup>[166]</sup> For further reading on hybrid MD/CFD approaches, we refer the interested reader to reviews such as refs. [6,167–171].

Let us conclude this section with two triple-scale approaches concurrently coupling atomistic, CG, and continuum approaches. In the first one, combining AdResS and a flux-exchange hybrid MD/CFD method,<sup>[155]</sup> insertion of complex molecules to match the mass and momentum fluxes at the particle and continuum interface is made feasible by implementing there a low resolution model (blob-molecules with soft effective interactions) and then using the AdResS to reintroduce the atomistic degrees of freedom and further couple with the bulk MD.<sup>[156,157]</sup> In the second one, coined the Triple-decker,<sup>[107,172]</sup> the state-variable coupling approach with the “handshaking” of the particle and continuum physical descriptions is used instead to couple atomistic and mesoscopic hydrodynamics.

## 4. AdResS and Open Systems Models

The coupling of an atomistic MD to an FHD simulation confronts us with the problem of a vast mismatch in the number of determining degrees of freedom between the two mathematical

models. This problem is familiar from any computational multiscale approach and a range of methods have been proposed to bridge this divide as summarized in Section 3 above. Here, we discuss one more specific issue arising when atomistic MD is coupled to FHD represented through finite volume or finite element discretizations, as opposed to coarse-grained or dissipative or other mesoscale particle-based representations.

In the context of the authors’ cooperation, we are interested specifically in coupling a finite-volume discretization of FHD to an atomistic thermostat-free Hamiltonian MD on a subdomain that interfaces with one or more of the FHD control volumes. In particular, we intend to allow for non-equilibrium situations with persistent, possibly non-steady, fluxes of mass, momentum, or energy through the atomistically resolved region maintained by gradients in the surrounding flow state. In this situation, each FHD control volume that interfaces with the AT region comes with its own independent flow state. The coupling of the two models should then be realized locally on each such interface and it should amount to constraining the atomistic MD simulation to concur with the FHD fluid state at the interface as monitored from the side of the FHD grid. The FHD simulation, in turn, should see interface-averaged mass, momentum, and energy fluxes—including their fluctuations – compatible with their particle-based analogues as determined from the MD side of the interface. We discuss part of the problem of constraining the MD simulation to match the FHD statistical moments in this section.

The most straightforward setting arises when the FHD subdomain is in thermodynamic equilibrium so that, after a short time, the MD domain should faithfully represent an “open molecular system” in the thermodynamic sense adhering to Grand Canonical statistics.<sup>[6,7,104,105]</sup> MD particles should be able to traverse the AT-domain’s interfaces in both directions thereby generating mean fluxes, including their fluctuations, that are compatible with the statistics of the outer equilibrium state. Two of the authors have recently proposed a mathematical formalization of this situation.<sup>[8]</sup> The goal in doing so was to highlight what is the information mismatch between the MD and FHD representations of the flow state and to suggest related plausible closures.

### 4.1. The Bergmann–Lebowitz (1955) Model

#### 4.1.1. Bergmann–Lebowitz Model Structure

The Bergmann–Lebowitz (BL) model of open system<sup>[173,174]</sup> is based on the idea that the coupling between the system and the reservoir/environment consists of an impulsive interaction at discrete points in time. Such an interaction, while interfering with the physics of the system, leaves the reservoir statistically undisturbed. In other words the macroscopic thermodynamic variables of the reservoir are not influenced by the behaviour of the system and the particles which enter into the system from the reservoir can only have velocities consistent with the temperature of the reservoir in thermal equilibrium. A suitable kernel,  $K_{nr}(X'_n, X_n)$ , formalizes mathematically such an interaction and corresponds to the probability per unit time that the system at  $X_n$  makes a transition to  $X'_n$ , caused by the interaction between the system and the



reservoir. The system-reservoir interaction is then reduced to:  $\sum_{n'=0}^{\infty} \int dX'_{n'} [K_{nn'}(X_n, X'_{n'}) f_{n'}(X'_{n'}, t) - K_{n'n}(X'_{n'}, X_n) f_n(X_n, t)]$ . The evolution in time of the phase-space probability of the system,  $f_n(X_n, t)$ , leads to a standard Liouville equation for a closed system, but augmented by the system-reservoir exchange term:

$$\frac{\partial f_n(X_n, t)}{\partial t} = \{f_n(X_n, t), H(X_n)\} + \sum_{n'=0}^{\infty} \int dX'_{n'} [K_{nn'}(X_n, X'_{n'}) f_{n'}(X'_{n'}, t) - K_{n'n}(X'_{n'}, X_n) f_n(X_n, t)] \quad (75)$$

In this context, the condition of flux balance expresses the condition of equilibrium:

$$\sum_{n'=0}^{\infty} \int dX'_{n'} [K_{nn'}(X_n, X'_{n'}) f_{n'}(X'_{n'}, t) - K_{n'n}(X'_{n'}, X_n) f_n(X_n, t)] = 0 \quad (76)$$

whose stationary solution for  $f_n(X_n)$  corresponds to the Grand Canonical probability density:  $f_n(X_n) = \frac{1}{\mathcal{Q}} e^{-\beta H_n(X_n) + \beta \mu n}$  where  $\beta = 1/k_B T$  and  $\mu$  the chemical potential.

#### 4.1.2. Relation to the AdResS Scheme and Design of Mean-Field Particle Reservoir

The AdResS scheme as an open system algorithm can be qualitatively mapped onto the BL model under the approximation that the reservoir is large enough to not be influenced by the AT region and that the interaction energy between the particles in the AT region and the particles in the reservoir (transition plus CG region) is negligible compared to the interaction energy among the particles of the atomistic region only.<sup>[5,7,175]</sup> In this context, AdResS offers a technical platform for the numerical treatment of open systems in a Grand Canonical-like fashion. Furthermore, as discussed above, the BL model defines a Liouville operator of a subsystem augmented by a stochastic kernel for describing the proper exchange of energy and particles with a reservoir. A relevant consequence is that such a mapping, despite being qualitative, is useful in defining relevant physical quantities such as time correlation functions of a subsystem embedded in a reservoir, this means a physical definition which allows direct comparisons with experimental data.<sup>[5,106,176,177]</sup> Within the setting of open system simulations, the technical set up of AdResS can be simplified further, and the use of the switching function  $w$  for the coupling can be removed, leading to a direct coupling and an abrupt change of resolution (See panel (b) of Figure 1). One of the advantages of such an approach would be to make  $F^{\text{AdResS}}$  conservative as in the Hamiltonian version of AdResS (H-AdResS)<sup>[103,178–182]</sup> but without violating the linear momentum conservation.<sup>[7]</sup> We have recently investigated ramifications of such a possibility in ref. [183] and provide a brief summary here.

Let us define  $d$ , the cut-off distance of molecular interactions. In the AT region, all molecules interact via the atomistic potential:  $V^{\text{AT}} = \sum_{(\alpha, \beta) \in \text{AT}} V^{\text{AT}}(\mathbf{r}_{\alpha}, \mathbf{r}_{\beta})$ , with  $V^{\text{AT}}(\mathbf{r}_{\alpha}, \mathbf{r}_{\beta})$  the AT potential between all the atoms  $\mathbf{r}_{\alpha}, \mathbf{r}_{\beta}$  of molecule  $\alpha$  and molecule  $\beta$ . In the CG region, all molecules interact via a CG potential:  $V_{\text{CG}} = \sum_{(\alpha, \beta) \in \text{CG}} V^{\text{CG}}(\mathbf{r}_{\alpha}, \mathbf{r}_{\beta})$ , with  $V^{\text{CG}}(\mathbf{r}_{\alpha}, \mathbf{r}_{\beta})$  the CG potential between the centers of mass  $\mathbf{r}_{\alpha}, \mathbf{r}_{\beta}$  of molecule  $\alpha$  and molecule  $\beta$ .

In the AT region next to the HY interface AT molecules interact with CG molecules via the CG potential. Since CG molecules do not have atomistic degrees of freedom there is no other way to interact with AT molecules:  $V_{\text{HY}}^{\text{coupling}} = \sum_{\alpha \in \Delta} \sum_{\beta \in \text{CG}} V^{\text{CG}}(\mathbf{r}_{\alpha}, \mathbf{r}_{\beta})$ , with  $\mathbf{r}_{\alpha}$  the center of mass of the atomistic molecule  $\alpha$  and  $\mathbf{r}_{\beta}$  the center of mass of the CG molecule  $\beta$ . Effectively, the HY region acts similarly to the transition region of standard AdResS. Thus, atomistic molecules closer to the CG region experience the CG character of the interaction more than AT molecules located at larger distance from the CG region; that is the passage from one resolution to the other is not artificially smoothed via  $w(r)$  as in standard AdResS, but it is implicitly gradual (i.e., function of  $r$ , not strictly abrupt). As in the standard AdResS, in the HY domain, we define  $F_{\alpha}^{\text{TD}}$  for the density balance.

Note that one of the aims of the switching function  $w$  in combination with the repulsive force capping and the local thermostat in the standard AdResS is to avoid fatal large forces due to potential overlaps (or nonphysical short distances) between atoms of neighboring molecules at the CG/HY interface. In the abrupt version, the overlaps must be avoided in another way, for example, by fixing the center of mass of a problematic molecule and running a few MD steps with a repulsive force capping to find an energetically permissible orientation. In a Monte-Carlo simulation, for example, this would be automatically taken care of by the rejection criterion.<sup>[100]</sup> Conceptually, this should be equivalent to the standard approach with the Heaviside step function used as the switching function  $w$  supplemented with the molecular orientation adjustment. The reason of the success of an abrupt approach lies in the fact that the formal criteria for defining an open system are not violated in a significant manner by the abrupt coupling and thus the method becomes more efficient.<sup>[175]</sup> Finally, an even more drastic simplification of the model of Krekeler et al.,<sup>[183]</sup> in closer connection to the idea of open system embedded in a generic thermodynamic reservoir was pursued recently.<sup>[123,184]</sup> Here, the CG region is substituted by a reservoir of non-interacting point-particle (tracers). The AT region exchanges particles and energy with the reservoir in an adaptive manner as in the standard AdResS (see panel (c) of Figure 1).

Another example of combining AdResS with a mass, momentum, and energy reservoir and imposing a local pressure tensor and a heat flux across the boundaries,<sup>[185]</sup> thus enabling Grand Canonical MD simulations, is provided by Open Boundary Molecular Dynamics (OBMD) method.<sup>[6,70,115–117]</sup>

## 4.2. n-Particle Hierarchy of Open System Liouville Equations

### 4.2.1. A Formalization of the Notion of “Open System”

Figure 2 shows a sketch of an open system (OS) as part of the “universe” (U). The environment of the open system (U\OS) is called the “outside world” below. We are interested in capturing the dynamics of OS as faithfully as possible, including the Hamiltonian nature of the detailed dynamics of the entire universe. Yet, by definition we have only limited statistical thermodynamic information regarding the latter, and the best we can therefore expect to do with respect to describing the open system’s evolution is to describe statistical features of its Hamiltonian

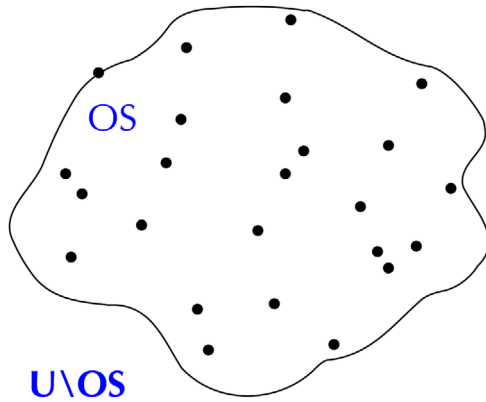


**Figure 2.** Sketch of an open system (OS) and its environment, called the “outside world.” The entire system, called “universe,”  $U$ , is supposed to include at total of  $N$  particles, to be closed in the far distance, and to be in canonical statistical equilibrium. The degrees of freedom of the particle in the universe are integrated out.

dynamics conditioned upon the canonical equilibrium statistics of the outside world.

The time evolution of the statistical distribution of an ensemble of universes under Hamiltonian dynamics,  $f(t, \mathbf{X}_N)$ , is governed by the  $N$ -particle Liouville equation,

$$\frac{\partial f(t, \mathbf{X}_N)}{\partial t} + \sum_{i=1}^N (\nabla_{q_i} \cdot (v_i f) + \nabla_{p_i} \cdot (F_i f))(t, \mathbf{X}_N) = 0 \quad (77)$$

Here,  $\mathbf{X}_N = [X_1, \dots, X_N] = [(q_1, p_1), \dots, (q_N, p_N)]$  is the  $N$ -particle state of the system with  $(q_i, p_i) \in U \times \mathbb{R}^3$  the position and momentum of the  $i$ th particle. Furthermore,  $v_i$  is  $i$ th particle's velocity, and  $F_i = -\partial H / \partial q_i$  the force acting upon it. In the definition of  $F_i$ , we are referring to the Hamiltonian,  $H(\mathbf{X}_N)$ , of the system. Note that we have consciously not adopted the standard notation for this equation utilizing the Poisson bracket, that is,  $f_t = \{f, H\} = H_{p_i} f_{q_i} - H_{q_i} f_{p_i}$ , to emphasize the character of the equation of a hyperbolic advection equation in state space.

Only some  $n \leq N$  particles reside in OS at any given time  $t$ , and we are only interested in monitoring the probability distribution for finding  $n$  particles near some state  $\mathbf{X}_n = (\mathbf{q}_n, \mathbf{p}_n)$  with  $\mathbf{q}_n \in \Omega^n$  and  $\Omega \subset \mathbb{R}^3$  being the spatial domain of the open system. More specifically, we are interested in the marginal distributions

$$f_n(t, \mathbf{X}_n) = B(n, N) \int_{(S^c)^{N-n}} f(t, \mathbf{X}_n, \Xi_{N-n}) d^{N-n} \Xi \quad (78)$$

where  $S^c = \Omega^c \times \mathbb{R}^3$ ,  $\Omega^c = U \setminus \Omega$ , and  $B(n, N)$  is the normalizing binomial coefficient that is introduced to account for the indistinguishability of the particles and that guarantees the normalization condition

$$\sum_{n=1}^N \int_{S^n} f_n(t, \mathbf{X}_n) d^n \mathbf{X} = 1 \quad (79)$$

Considering the full Liouville equation separately for states featuring  $1, 2, \dots, n, \dots, N$  particles within the OS domain  $\Omega$ , and integrating the degrees of freedom of the remaining  $N - n$  parti-

cles, the following hierarchy of  $n$ -particle Liouville equations can be derived,<sup>[8]</sup>

$$\frac{\partial f_n}{\partial t} + \sum_{i=1}^n (\nabla_{q_i} \cdot (p_i f_n) + \nabla_{p_i} \cdot (F_i f_n)) = \Phi_n^{n+1} + \Psi_n \quad (80)$$

where the terms on the left correspond to the Liouville equation for the Hamiltonian dynamics of  $n$  particles residing within the OS domain alone. The terms on the right represent the coupling of the  $(n + 1)$ - and  $n$ -particle distributions due to passage of particles across the interface of the OS domain,

$$\begin{aligned} \Phi_n^{n+1} = (n + 1) \int_{\partial \Omega} \int_{(p_i \cdot \mathbf{n}) > 0} (p_i \cdot \mathbf{n}) f_{n+1}(t, \mathbf{X}_n, (q_i, p_i)) \\ - f_n(t, \mathbf{X}_n) f_1^\circ(q_i, -p_i) d^3 p_i d\sigma_i \end{aligned} \quad (81)$$

and the mean forcing of the particles inside the OS domain by those in the outside world, that is, the ensemble averaged action of the outside particles onto the particle inside,

$$\Psi_n = - \sum_{i=1}^n \nabla_{p_i} \cdot \left( F_{av}(q_i) f_n(t, \mathbf{X}_{i-1}, X_i, \mathbf{X}_{n-i}) \right) \quad (82)$$

with

$$F_{av}(q_i) = - \int_{S^c} \nabla_{q_i} V(q_i - q_j) f_2^\circ(X_j | X_i) dX_j \quad (83)$$

In Equation (81) the quantity  $f_1^\circ(q_i, -p_i)$  is the single-particle distribution function of the outside world, while in Equation (83) the quantity  $f_2^\circ(X_j | X_i)$  is the outside world single-particle distribution for particle  $j$  conditioned upon the state of the  $i$ th particle.

The manipulations leading from Equations (77) to (78)–(83) are straightforward. In only two places it is necessary to implement closure assumptions or, equivalently, explicit modeling of the properties of the outside world.<sup>[8]</sup> The first is manifest in Equation (81) where, after integration of the physical space divergence terms  $\nabla_{q_i} \cdot (p_i f)$  over the outside world domain  $\Omega^c$ , we have to distinguish which information regarding the probability densities is transported into  $(p_i \cdot \mathbf{n} < 0)$  and out of  $(p_i \cdot \mathbf{n} > 0)$  the open system. When a particle exits the open system, so that afterward there are  $n$  particles left inside, then it transports the corresponding  $(n + 1)$ -particle state space density (first term in the integral). In contrast, the second term represents the net influx of probability from the outside world equilibrium.

In formulating this latter term it was assumed that the outside world single-particle marginal density  $f_1^\circ$  is independent of the current state in the open system.<sup>[8]</sup> A similar assumption was introduced to model the net forcing of particles inside the system by those residing outside of it. Alternative physically meaningful closures are conceivable and will be at the focus of future work, especially in the context of non-equilibrium dynamics, where the statistical closure assumptions will have to have a local character depending on the position along the open system's interface.

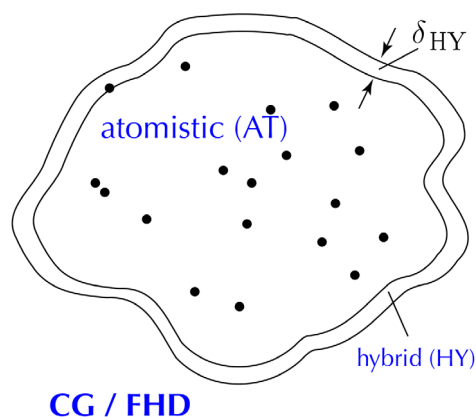


**Figure 3.** Sketch of an open system modelled by the AdResS approach. The hybrid region shields the particles inside the open system from the detailed properties of those in the outside world. As a consequence, the latter can be treated as non-interacting point-particles embedded in a mean-field (tracers) with the technical convenience of not requiring a process of insertion and deletion in the high resolution region.

#### 4.2.2. Relation to the AdResS Scheme

The open system description of the previous section is conceptually very close to the AdResS model paradigm. In fact, inside the atomistically resolved region AT (see **Figure 3**) the model imposes Hamiltonian dynamics of the particles. It couples the AT region to thermostatted and externally forced atomistic Hamiltonian dynamics in the HY. The latter, in turn, communicates with the outside world. Forcings and interactions in the hybrid region are designed to prepare the statistics of particles near the AT-HY-interface to closely approximate a local statistical equilibrium. Particles exiting or entering the AT region therefore carry approximately the internal or externally prepared statistics across the interface, respectively, as expressed by the particle exchange term  $\Phi_n^{n+1}$  from Equation (81).

Particles residing next to the interface but inside the AT domain “feel” the potential interaction force from close-by particles in the HY. With these being forced to adhere to an externally determined statistics, they exert in the temporal mean a mean-field force similar to that implied by the momentum forcing term  $\Psi_n$  in Equation (82).

The modeling of an open system in non-equilibrium would be modeled analogously, yet the statistical information imposed along the boundary of the OS domain would be determined by the hydrodynamic states within grid boxes of a finite volume FHD simulation that are intersected by that surface as sketched in **Figure 4**.

## 5. Discussion about Scaling Regimes and Derivation of Coupling Strategies

In the construction of an MD-FHD hybrid model, several issues of “scaling” need to be addressed. FHD is intended to represent mesoscopic scales that are small enough for thermal fluctuations to play a significant role in the dynamics while being large enough for fluctuations to be representable

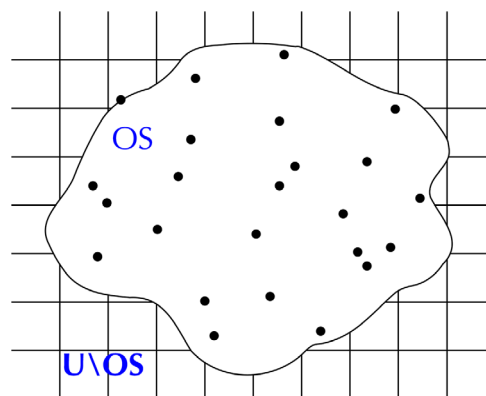


**Figure 4.** Sketch of an open non-equilibrium system modelled by the AdResS approach coupled to a grid-based fluctuating hydrodynamics code.

by a Markovian approximation with Gaussian noise. The observed covariance of fluctuations in a fluid scales inversely with the volume used to measure the covariance.<sup>[47]</sup> The smaller the region over which the variance is computed, the larger the variance. In finite volume-based FHD computational models, this is reflected in how the stochastic fluxes scale with cell volume.<sup>[186]</sup> (In finite volume FHD stochastic fluxes are scaled by  $1/\sqrt{\Delta t V}$  to match the space-time integration of  $\delta$  correlated noise over the space-time discretization element.) Assuming the fluctuations can be represented with a Markovian approximation with Gaussian noise implicitly assumes a separation of scales between the FHD representation and molecular scales. This can most easily be thought of in terms of number of molecules per cell. If the number of molecules per cell becomes too small, one expects the assumptions underlying FHD to begin to break down. Fluxes will no longer be accurately represented by Gaussians and memory effects may become important.

Bian et al.<sup>[62]</sup> study deviations from the continuum limit at meso-scales for time correlations obtained from detailed MD, from a heuristic and a Mori–Zwanzig CG version of DPD, and from linearized FHD. Quantitative estimates are provided for a specific star-polymer melt system. The authors find convincing agreement for time correlations of spatial Fourier modes of mass fluxes of all models at sufficiently large scales, i.e., in the continuum limit. Good quantitative agreement was achieved at wavelengths corresponding to just 5 to 10 times the average molecular distance or 125 to 1000 molecules in a box of that length scale. At meso-scales, that is, below a typical number of 125 molecules in a cube results from linearized FHD deviate substantially from those obtained by MD and coarse-grained DPD. All reduced models are Markovian, however, so that even at the considered meso-scales, memory effects seem unimportant. As particle numbers of 125 to 1000 are well within reach of MD simulations, it seems reasonable on the basis of these observations to aim for a direct coupling of MD and FHD as discussed in this report.

Considerations of fluctuation amplitude scaling yield an additional argument for direct MD-FHD coupling without an intermediate CG model. The central point of a CG model is a reduction of the number of effective degrees of freedom. As a consequence of the fluctuation scaling with the particle number

per grid box a CG model will, for a given grid resolution, imply larger fluctuation amplitudes on the side of the FHD model to which it is coupled than would its atomistic counterpart. It appears not clear a priori that two FHD models whose parameters are adjusted to match an atomistic and a coarse-grained model of the same fluid will automatically lead to identical statistics regarding the large fluctuations that they will singularly generate.

The FHD equations proposed by Landau and Lifshitz<sup>[35]</sup> and more elaborate nonlinear versions introduced subsequently<sup>[11]</sup> all involve terms representing divergences of stochastic spatially decorrelated fluxes. Mathematically speaking, such terms are meaningless when interpreted in the sense of sums of partial derivatives of the flux fields as the spatial decorrelation contradicts the existence of the appropriate limits of finite differences. This does not imply, however, that there should not be an interpretation of these terms in the sense of distributions. The search for a conceptually meaningful interpretation of these aspects has recently stimulated intense mathematical research at the forefront of stochastic analysis of partial differential equations.<sup>[187,188]</sup> Satisfactory answers to these questions are still pending, however.

## 6. Current and Future Representative Examples of Application

In this section, we briefly describe some examples of numerical applications from current and future research projects that highlight how the theoretical apparatus described above can be translated into relevant computational tools. The examples are taken from materials science (star polymer melt under shear), nanotechnology (charge transport), and physical chemistry (ionic liquids). In each case, there is across-scale information flow such that coupling of specific local chemistry to the meso and macroscales is required.

### 6.1. Star Polymer Melt under Shear

OBMD mentioned earlier allows for equilibrium MD simulations in the Grand Canonical ensemble as well as nonequilibrium fluid flow simulations by introducing the flow via an external boundary condition while the equations of motion for the bulk remain unaltered. One example for which the OBMD method excels, is a star polymer melt under shear.<sup>[6, 115–117]</sup> It is a representative OBMD system that sees molecules freely flow inward or outward of the simulation box according to the externally imposed thermo-mechanical state. The simulation box is composed of a central MD domain sandwiched between two buffer domains. The latter allow the central box to exchange mass, momentum, and energy through two of its boundaries with the buffers. The system is opened in this direction and star polymers freely move between different domains. Additionally, in the buffers, a change of resolution takes place from the fine (next to the central MD domain) to the coarser resolution (at the outer boundaries of the simulation box). In the CG parts of the buffers, a given molecule is represented by only one soft CG bead. The idea behind the resolution change in the buffers is that AdResS allows the insertion of molecules of arbitrary size into the system. The CG domains

of the buffers act as a mass reservoir into which large molecules can be easily inserted due to weak effective interactions among the soft beads. As the molecules move toward the MD domain, they gain the fine-grained details according to the AdResS strategy. Molecules are deleted once they leave the outer boundary of a given buffer and new molecules are inserted to achieve the mass balance.

### 6.2. From Quantum Chemistry to Continuum: Charge Transport and Ionic Liquids

A frontier in the development of across-scale coupling schemes in molecular science concerns computational treatments from quantum up to hydrodynamic scales. Some examples were mentioned in Section 1. A typical example is the flow of electrons through a junction that connects two electrodes. This is a classical example of a multiscale problem in which the local chemistry of the junction, usually a molecule, is intimately linked to the local chemistry of the surface of the electrode to which the molecule is attached, and to the global arrangement of the large scale structure of the electrode in the bulk. Typically, the bulk of the electrode is treated as a continuum representing a reservoir from which electrons flow into the junction whose specific chemical properties in turn determine the electronic characteristics, that is, the technological quality, of the device.

The injection of electrons into the chemically resolved junction molecule occurs through a hopping matrix derived by its electronic states through quantum calculations of such a subsystem. The hopping matrix is used to determine at each step whether an electron is injected into the junction or is adsorbed by the bulk of the second electrode, and this creates a net electron current. Latest developments involve more directly the full electron dynamics by treating the Liouville equation for the Density Matrix of the electronic states of the junction. The environment/bulk (reservoir) is treated very closely to the methods of hydrodynamics reported here and the description of the subsystem of interest makes use of the projection operator formalism of section 2.3.4. Details of such an approach can be found in ref. [189] (and references therein).

Further examples of linking the macro, meso, atomistic, and electronic scale arise in physical chemistry when, at a microscale, one might be interested in the local solvation properties of a liquid, whereas at a macroscale one considers the thermodynamic properties of such a liquid. Technological applications include lubrication and electronic transport in electrolytes. The field of ionic liquids is a further example. Ionic liquids are composed of cations and anions which keep neutrality globally but locally exhibit all characteristics of ionic solutions. This field of study is continuously growing because the rational on demand design of molecules with particular properties has led to substances with properties of high technological interest, although the scientific understanding of links between the specific chemistry of the molecules and their hydrodynamic properties remains limited today.<sup>[190]</sup> In fact, while at the electronic-atomistic scales simulations are already possible through the so-called QM/MM methods,<sup>[191]</sup> which consider a quantum subsystem embedded in an atomistic environment, studies that connect the microscopic scale with the hydrodynamic scale are part of future



research projects. In this perspective, the AdResS methodology has already and successfully treated ionic liquids at classical level<sup>[192–194]</sup> and thus a next step in the direction of the hydrodynamic scale would be to link the tracer region of AdResS to a continuum description. In the other direction, that is from the atomistic to the electronic scale, the latest development of AdResS, el-QM-AdResS, which describe a Grand Canonical electronic system embedded in a classical atomistic reservoir,<sup>[195]</sup> represents a tool for simulating local specific electronic properties in a larger atomistic environment. Thus, in principle the required technology to span simultaneously all the scales involved is available and future projects will hopefully realize their sound coupling and exploitation.

## 7. Conclusions

The coupling of particle-based approaches to the continuum technique has been discussed by summarizing the state of the art in the field and by organizing it in such a way that physical models are followed by the corresponding mathematical formalization which in turn leads to numerical implementations and finally to applications in which atomistic-scale processes are crucially influenced by large-scale fluid properties and vice versa. Advantages and limitations of the physical models and/or approximations which allow for feasible mathematical derivations of equations that govern physical observables as a function of the degrees of freedom of the problem, have been discussed and put in perspective; open problems are proposed as potential research projects for the next years.

## Acknowledgements

M.P. acknowledges financial support through grant P1-0002 from the Slovenian Research Agency. L.D.S. and R.K. acknowledge the support of Deutsche Forschungsgemeinschaft through the Collaborative Research Center CRC 1114 “Scaling Cascades in Complex Systems”, project C01. J.B.B. was supported by the U.S. Department of Energy, Office of Science, Office of Advanced Scientific Computing Research, Applied Mathematics Program under contract DE-AC02-05CH11231.

Correction added on 4th February, after first online publication: Projekt Deal funding statement has been added.

Open access funding enabled and organized by Projekt DEAL.

## Conflict of Interest

The authors declare no conflict of interest.

## Keywords

fluid dynamics, molecular dynamics, multiscale simulations

Received: November 25, 2019

Revised: February 11, 2020

Published online: March 19, 2020

[1] A. Prajapati, M. R. Singh, *ACS Sustainable Chem. Eng.* **2019**, 7, 5993.

[2] D. A. Fedosov, A. Sengupta, G. Gompper, *Soft Matter* **2015**, 11, 6703.

[3] R. Schmitz, *Phys. Rep.* **1988**, 171, 1.

- [4] A. Donev, E. Vanden-Eijnden, A. Garcia, J. Bell, *Commun. Appl. Math. Comput. Sci.* **2010**, 5, 149.
- [5] A. Agarwal, J. Zhu, C. Hartmann, H. Wang, L. Delle Site, *New J. Phys.* **2015**, 17, 083042.
- [6] R. Delgado-Buscalioni, J. Sablić, M. Praprotnik, *Eur. Phys. J. Special Topics* **2015**, 224, 2331.
- [7] L. Delle Site, M. Praprotnik, *Phys. Rep.* **2017**, 693, 1.
- [8] L. Delle Site, R. Klein, **2019**, submitted, arXiv:1907.07557.
- [9] L. Boltzmann, *Über die Prinzipien der Mechanik: Zwei Akademische Antrittsreden*, S. Hirzel, Leipzig **1903**.
- [10] H. Grabert, *Projection Operator Techniques in Non-Equilibrium Statistical Mechanics*, Vol. 95, Springer, Berlin, Heidelberg **1982**.
- [11] P. Espanol, *Phys. A* **1998**, 248, 77.
- [12] R. Zwanzig, *Nonequilibrium Statistical Mechanics*, Oxford University Press, New York **2001**.
- [13] F. Golse in *The Boltzmann Equation and its Hydrodynamic Limits*, Vol. 2 (Ed.: E. F. C. Dafermos), Elsevier, Amsterdam **2005**, Ch. 3, p. 1.
- [14] L. Saint-Raymond, *Hydrodynamic Limits of the Boltzmann Equation*, Vol. 1971, Springer, Berlin, Heidelberg **2009**.
- [15] I. Gallagher, *Bull. Am. Math. Soc.* **2019**, 56, 65.
- [16] W. G. Noid, *J. Chem. Phys.* **2013**, 139, 090901.
- [17] Z. Li, X. Bian, X. Yang, G. Karniadakis, *J. Chem. Phys.* **2016**, 145, 044102.
- [18] M. Praprotnik, L. Delle Site, K. Kremer, *Annu. Rev. Phys. Chem.* **2008**, 59, 545.
- [19] H. Wang, C. Junghans, K. Kremer, *Eur. Phys. J. E* **2009**, 28, 221.
- [20] M. S. Green, *J. Chem. Phys.* **1954**, 22, 398.
- [21] R. Kubo, *J. Phys. Soc. Jpn.* **1957**, 12, 570.
- [22] A. Popadić, D. Sveneš, R. Podgornik, M. Praprotnik, *Adv. Theory Simul.* **2019**, 2, 1900019.
- [23] D. Violeau, B. D. Rogers, *J. Hydraulic Res.* **2016**, 54, 1.
- [24] P. Español, P. B. Warren, *J. Chem. Phys.* **2017**, 146, 150901.
- [25] A. Donev, A. Garcia, B. Alder, *J. Stat. Mech. Theory Exp.* **2009**, P11008.
- [26] H. Yserentant, *Numer. Math.* **1997**, 76, 111.
- [27] S. Chen, G. D. Doolen, *Annu. Rev. Fluid Mech.* **1998**, 30, 329.
- [28] A. L. Garcia, M. M. Mansour, G. C. Lie, E. Clementi, *J. Stat. Phys.* **1987**, 47, 209.
- [29] D. Bruno, *Phys. Fluids* **2019**, 31, 047105.
- [30] N. K. Voulgarakis, J. W. Chu, *J. Chem. Phys.* **2009**, 130, 134111.
- [31] B. Z. Shang, N. K. Voulgarakis, J. W. Chu, *J. Chem. Phys.* **2011**, 135, 044111.
- [32] A. Donev, J. B. Bell, A. L. Garcia, B. J. Alder, *SIAM J. Multiscale Modeling and Simulation* **2010**, 8, 871.
- [33] P. Español, H. C. Öttinger, *Z. Phys. B* **1993**, 90, 377.
- [34] A. J. Chorin, O. H. Hald, R. Kupferman, *PNAS* **2000**, 97, 2968.
- [35] L. Landau, E. Lifshitz, *Fluid Mechanics*, Pergamon Press, Oxford **1959**.
- [36] J. Smoller, *Shock Waves and Reaction–Diffusion Systems*, 2nd ed., Vol. 258, Springer, Berlin **1994**.
- [37] R. J. LeVeque, *Finite Volume Methods for Hyperbolic Problems*, Cambridge University Press, Basel **2002**.
- [38] D. Zubarev, V. Morozov, *Physica A* **1983**, 120, 411.
- [39] C. Gardiner, *Handbook of Stochastic Methods*, Springer Verlag, Berlin **2002**.
- [40] J. O. Hirschfelder, C. F. Curtiss, R. B. Bird, *Molecular Theory of Gases and Liquids*, John Wiley and Sons, INC., New York **1954**.
- [41] C. Cohen, J. W. H. Sutherland, J. M. Deutch, *Phys. and Chem. of Liquids* **1971**, 2, 213.
- [42] B. Law, J. Nieuwoudt, *Phys. Rev. A* **1989**, 40, 3880.
- [43] J. Nieuwoudt, B. Law, *Phys. Rev. A* **1989**, 42, 2003.
- [44] J. M. O. de Zarate, J. V. Sengers, *Hydrodynamic Fluctuations in Fluids and Fluid Mixtures*, Elsevier Science, Oxford **2007**.



- [45] J. M. O. de Zárte, J. L. Hita, J. V. Sengers, C. R. Mec. **2013**, 341, 399.
- [46] H. C. Öttinger, *The J. Chem. Phys.* **2009**, 130, 114904.
- [47] K. Balakrishnan, A. L. Garcia, A. Donev, J. B. Bell, *Phys. Rev. E* **2014**, 89, 013017.
- [48] A. Donev, A. J. Nonaka, A. K. Bhattacharjee, A. L. Garcia, J. B. Bell, *Phys. Fluids* **2015**, 27, 037103.
- [49] S. R. DeGroot, P. Mazur, *Non-Equilibrium Thermodynamics*, North-Holland Publishing Company, Amsterdam **1963**.
- [50] L. D. Landau, E. M. Lifshitz, *Fluid Mechanics, Course of Theoretical Physics*, Vol. 6, Pergamon Press, Oxford **1959**.
- [51] G. D. C. Kuiken, *Thermodynamics of Irreversible Processes: Applications to Diffusion and Rheology*, Wiley, New York **1994**.
- [52] V. Giovangigli, *Multicomponent Flow Modeling*, Birkhauser Boston **1999**.
- [53] D. T. Gillespie, *J. Chem. Phys.* **2000**, 113, 297.
- [54] A. Bhattacharjee, K. Balakrishnan, A. Garcia, J. Bell, A. Donev, *J. Chem. Phys.* **2015**, 142, 224107.
- [55] D. T. Gillespie, *J. Computation. Phys.* **1976**, 22, 403.
- [56] D. T. Gillespie, *J. Chem. Phys.* **2001**, 115, 1716.
- [57] C. Kim, A. Nonaka, J. Bell, A. Garcia, A. Donev, *J. Chem. Phys.* **2017**, 146, 124110.
- [58] C. Kim, A. Nonaka, J. Bell, A. Garcia, A. Donev, *J. Chem. Phys.* **2018**, 149, 084113.
- [59] P. Español, J. G. Anero, I. Zúñiga, *J. Chem. Phys.* **2009**, 131, 244117.
- [60] P. Español, A. Donev, *J. Chem. Phys.* **2015**, 143, 234104.
- [61] N. K. Voulgarakis, S. Satish, J. W. Chu, *J. Chem. Phys.* **2009**, 131, 234115.
- [62] X. Bian, Z. Li, N. Adams, *Appl. Math. Mech. (Engl. Ed.)* **2018**, 39, 63.
- [63] B. Shadrack Jabes, R. Klein, L. Delle Site, *Adv. Theory Simul.* **2018**, 1, 1800025.
- [64] P. M. J. Trevelyan, C. Almarcha, A. D. Wit, *J. Fluid Mech.* **2011**, 670, 38.
- [65] M. P. Allen, D. J. Tildesley, *Computer Simulation of Liquids*, Clarendon Press, Oxford **1989**.
- [66] B. J. Alder, T. E. Wainwright, *J. Chem. Phys.* **1959**, 31, 459.
- [67] M. E. Tuckerman, *Statistical Mechanics: Theory and Molecular Simulation*, Oxford University Press, New York **2010**.
- [68] J. Zavadlav, R. Podgornik, M. Praprotnik, *Sci. Rep.* **2017**, 7, 4775.
- [69] J. Zavadlav, S. J. Marrink, M. Praprotnik, *Interface Focus* **2019**, 9, 20180075.
- [70] J. Zavadlav, J. Sablić, R. Podgornik, M. Praprotnik, *Biophys. J.* **2018**, 114, 2352.
- [71] *Coarse-Graining of Condensed Phase and Biomolecular Systems* (Ed.: G. A. Voth), CRC Press, Boca Raton **2008**.
- [72] *Coarse-Grained Modeling of Biomolecules* (Ed.: G. A. Papoian), CRC Press, Boca Raton **2017**.
- [73] W. G. Noid, *J. Chem. Phys.* **2013**, 139, 090901.
- [74] S. Izvekov, M. Parrinello, C. B. Burnham, G. A. Voth, *J. Chem. Phys.* **2004**, 120, 10896.
- [75] S. Izvekov, G. A. Voth, *J. Chem. Phys.* **2005**, 123, 134105.
- [76] M. S. Shell, *J. Chem. Phys.* **2008**, 129, 144108.
- [77] T. Foley, M. S. Shell, W. G. Noid, *J. Chem. Phys.* **2015**, 143, 243104.
- [78] M. Langenberg, N. E. Jackson, J. J. de Pablo, M. Müller, *J. Chem. Phys.* **2018**, 148, 094112.
- [79] A. P. Lyubartsev, A. Naðmé, D. P. Vercauteren, A. Laaksonen, *J. Chem. Phys.* **2015**, 143, 243120.
- [80] G. Kihara, Y. Yoshimoto, T. Hori, S. Takagi, I. Kinefuchi, *Trans. Jpn. Soc. Mech. Eng.* **2018**, 84, 18.
- [81] M. G. Guenza, M. Dinpajoo, J. McCarty, I. Y. Lyubimov, *J. Phys. Chem. B* **2018**, 10.1021/acs.jpcc.8b0668.
- [82] Z. Li, X. Bian, B. Caswell, G. E. Karniadakis, *Soft Matter* **2014**, 10, 8659.
- [83] S. J. Marrink, D. P. Tieleman, *Chem. Soc. Rev.* **2013**, 42, 6801.
- [84] S. O. Yesylevskyy, L. V. Schäfer, D. Sengupta, S. J. Marrink, *PLoS Comput. Biol.* **2010**, 6, e1000810.
- [85] Z. Wu, Q. Cui, A. Yethiraj, *J. Phys. Chem. B* **2010**, 114, 10524.
- [86] S. Riniker, W. F. van Gunsteren, *J. Chem. Phys.* **2011**, 134, 084110.
- [87] L. Darré, M. R. Machado, P. D. Dans, F. E. Herrera, S. Pantano, *J. Chem. Theory Comput.* **2010**, 6, 3793.
- [88] M. R. Machado, H. C. González, S. Pantano, *J. Chem. Theory Comput.* **2017**, 13, 5106.
- [89] T. Ha-Duong, N. Basdevant, D. Borgis, *Chem. Phys. Lett.* **2009**, 79.
- [90] J. Zavadlav, G. Arampatzis, P. Koumoutsakos, *Sci. Rep.* **2019**, 9, 99.
- [91] R. D. Groot, P. B. Warren, *J. Chem. Phys.* **1997**, 107, 4423.
- [92] P. Español, *Phys. Rev. E* **1995**, 52, 1734.
- [93] P. J. Hoogerbrugge, J. M. V. A. Koelman, *Europhys. Lett.* **1992**, 19, 155.
- [94] P. Español, P. B. Warren, *Europhys. Lett.* **1995**, 30, 191.
- [95] E. K. Peter, I. V. Pivkin, *J. Chem. Phys.* **2014**, 141, 164506.
- [96] P. B. Warren, A. Vlasov, *J. Chem. Phys.* **2014**, 140, 084904.
- [97] R. D. Groot, *J. Chem. Phys.* **2003**, 118, 11265.
- [98] A. J. Rzepiela, M. Louhivuori, C. Peter, S. J. Marrink, *Phys. Chem. Chem. Phys.* **2011**, 13, 10437.
- [99] N. Goga, M. N. Melo, A. J. Rzepiela, A. H. de Vries, A. Hadar, S. J. Marrink, H. J. C. Berendsen, *J. Chem. Theory Comput.* **2015**, 11, 1389.
- [100] A. Cameron, *J. Chem. Phys.* **2005**, 123, 234101.
- [101] S. O. Nielsen, P. B. Moore, B. Ensing, *Phys. Rev. Lett.* **2010**, 105, 237802.
- [102] A. Heyden, D. G. Truhlar, *J. Chem. Theory Comput.* **2008**, 4, 217.
- [103] R. Potestio, S. Fritsch, P. Español, R. Delgado-Buscalioni, K. Kremer, R. Everaers, D. Donadio, *Phys. Rev. Lett.* **2013**, 110, 108301.
- [104] H. Wang, C. Schütte, L. Delle Site, *J. Chem. Theory Comput.* **2012**, 8, 2878.
- [105] H. Wang, C. Hartmann, C. Schütte, L. Delle Site, *Phys. Rev. X* **2013**, 3, 011018.
- [106] A. Agarwal, L. Delle Site, *J. Chem. Phys.* **2015**, 143, 094102.
- [107] D. A. Fedosov, G. E. Karniadakis, *J. Comput. Phys.* **2009**, 228, 1157.
- [108] R. Delgado-Buscalioni, *Phil. Trans. R. Soc. A* **2016**, 374, 20160152.
- [109] J. H. Walther, M. Praprotnik, E. M. Kotsalis, P. Koumoutsakos, *J. Comput. Phys.* **2012**, 231, 2677.
- [110] R. Erban, *Proc. R. Soc. A* **2016**, 472, 20150556.
- [111] N. D. Petsev, L. G. Leal, M. S. Shell, *J. Chem. Phys.* **2015**, 142, 044101.
- [112] U. Alekseeva, R. G. Winkler, G. Sutmann, *J. Comp. Phys.* **2016**, 314, 14.
- [113] A. Scutkins, D. Nerukh, E. Pavlov, S. Karabasov, A. Markesteyn, *Eur. Phys. J. Special Topics* **2015**, 224, 2217.
- [114] J. Krajniak, S. Pandiyan, E. Nies, G. Samaey, *J. Chem. Theory. Comput.* **2016**, 12, 5549.
- [115] J. Sablić, M. Praprotnik, R. Delgado-Buscalioni, *Soft Matter* **2016**, 12, 2416.
- [116] J. Sablić, M. Praprotnik, R. Delgado-Buscalioni, *Soft Matter* **2017**, 13, 4971.
- [117] J. Sablić, R. Delgado-Buscalioni, M. Praprotnik, *Soft Matter* **2017**, 13, 6988.
- [118] M. Praprotnik, L. Delle Site, K. Kremer, *J. Chem. Phys.* **2005**, 123, 224106.
- [119] M. Praprotnik, R. Cortes-Huerto, R. Potestio, L. Delle Site in *Handbook of Materials Modeling* (Eds.: W. Andreoni, S. Yip), Springer, Cham **2018**, p. 1.
- [120] S. Yasuda, R. Yamamoto, *Phys. Rev. X* **2014**, 4, 041011.
- [121] S. Stalter, L. Yelash, N. Emamy, M. Hanke, Lukáčová-Medvid'ová, *Comp. Phys. Comm.* **2018**, 224, 198.
- [122] M. Lee, F. Salsbury Jr., M. Olson, *J. Comp. Chem.* **2004**, 25, 1967.

- [123] L. Delle Site, K. Krekeler, J. Whittaker, A. Agarwal, R. Klein, F. Höfling, *Adv. Theory Simulat.* **2019**, 2, 1900014.
- [124] J. Zavadlav, M. Praprotnik, *J. Chem. Phys.* **2017**, 147, 114110.
- [125] J. Zavadlav, S. J. Marrink, M. Praprotnik, *J. Chem. Theory Comput.* **2016**, 12, 4138.
- [126] J. Zavadlav, R. Podgornik, M. Praprotnik, *J. Chem. Theory Comput.* **2015**, 11, 5035.
- [127] J. Zavadlav, M. N. Melo, S. J. Marrink, M. Praprotnik, *J. Chem. Phys.* **2014**, 140, 054114.
- [128] K. Kreis, R. Potestio, K. Kremer, A. C. Fogarty, *J. Chem. Theory Comput.* **2016**, 12, 4067.
- [129] S. Poblete, M. Praprotnik, K. Kremer, L. Delle Site, *J. Chem. Phys.* **2010**, 132, 114101.
- [130] M. Praprotnik, S. Poblete, K. Kremer, *J. Stat. Phys.* **2011**, 145, 946.
- [131] S. Fritsch, S. Poblete, C. Junghans, G. Ciccotti, L. Delle Site, K. Kremer, *Phys. Rev. Lett.* **2012**, 108, 170602.
- [132] T. Soddemann, B. Dünweg, K. Kremer, *Phys. Rev. E* **2003**, 68, 046702.
- [133] C. Junghans, M. Praprotnik, K. Kremer, *Soft Matter* **2008**, 4, 156.
- [134] J. Zavadlav, S. J. Marrink, M. Praprotnik, *J. Chem. Theory Comput.* **2018**, 14, 1754.
- [135] A. Popadić, J. H. Walther, P. Koumoutsakos, M. Praprotnik, *New J. Phys.* **2014**, 16, 082001.
- [136] A. Popadić, M. Praprotnik, P. Koumoutsakos, J. H. Walther, *Eur. Phys. J. Special Topics* **2015**, 224, 2321.
- [137] E. R. Cruz-Chú, E. Papadopolou, J. H. Walther, A. Popadić, G. Gengyun Li, M. Praprotnik, P. Koumoutsakos, *Nat. Nanotechnol.* **2017**, 12, 1106.
- [138] P. M. Kulkarni, C.-C. Fu, M. S. Shell, L. Gary Leal, *J. Chem. Phys.* **2013**, 138, 234105.
- [139] N. D. Petsev, L. G. Leal, M. S. Shell, *J. Chem. Phys.* **2016**, 144, 084115.
- [140] N. D. Petsev, L. G. Leal, M. S. Shell, *J. Chem. Phys.* **2017**, 147, 234112.
- [141] P. Español, M. Revenga, *Phys. Rev. E* **2003**, 67, 026705.
- [142] L. B. Lucy, *Astron. J.* **1977**, 82, 1013.
- [143] R. A. Gingold, J. J. Monaghan, *Mon. Not. R. Astron. Sci.* **1977**, 181, 375.
- [144] U. Alekseeva, R. G. Winkler, G. Sutmann, *J. Comput. Phys.* **2016**, 314, 14.
- [145] A. Malevanets, R. Kapral, *J. Chem. Phys.* **1999**, 110, 8605.
- [146] I. Korotkin, S. Karabasov, D. Nerukh, A. Markesteijn, A. Scukins, V. Farafonov, E. Pavlov, *J. Chem. Phys.* **2015**, 143, 014110.
- [147] J. Hu, I. A. Korotkin, S. A. Karabasov, *J. Chem. Phys.* **2018**, 149, 084108.
- [148] I. A. Korotkin, S. A. Karabasov, *J. Chem. Phys.* **2018**, 149, 244101.
- [149] S. T. O'Connell, P. A. Thompson, *Phys. Rev. E* **1995**, 52, R5792.
- [150] N. G. Hadjiconstantinou, *Phys. Rev. E* **1999**, 59, 2475.
- [151] X. Nie, S. Chen, M. O. Robbins, *Phys. Fluids* **2004**, 16, 3579.
- [152] X. Nie, M. O. Robbins, S. Chen, *Phys. Rev. Lett.* **2006**, 96, 134501.
- [153] T. Werder, J. H. Walther, P. Koumoutsakos, *J. Comput. Phys.* **2005**, 205, 373.
- [154] E. G. Flekkoy, G. Wagner, J. Feder, *Europhys. Lett.* **2000**, 52, 271.
- [155] G. D. Fabritiis, R. Delgado-Buscalioni, P. V. Coveney, *Phys. Rev. Lett.* **2006**, 97, 134501.
- [156] R. Delgado-Buscalioni, K. Kremer, M. Praprotnik, *J. Chem. Phys.* **2008**, 128, 114110.
- [157] R. Delgado-Buscalioni, K. Kremer, M. Praprotnik, *J. Chem. Phys.* **2009**, 131, 244107.
- [158] G. De Fabritiis, M. Serrano, R. Delgado-Buscalioni, P. V. Coveney, *Phys. Rev. E* **2007**, 75, 026307.
- [159] R. Delgado-Buscalioni, G. De Fabritiis, *Phys. Rev. E* **2007**, 76, 036709.
- [160] F. B. Usabiaga, I. Pagonabarraga, R. Delgado-Buscalioni, *J. Comput. Phys.* **2013**, 235, 701.
- [161] F. BalboaUsabiaga, J. Bell, R. Delgado-Buscalioni, A. Donev, T. Fai, B. Griffith, C. Peskin, *Multiscale Model. Simul.* **2012**, 10, 1369.
- [162] A. Donev, J. B. Bell, A. L. Garcia, B. J. Alder, *Multiscale Model. Simul.* **2010**, 8, 871.
- [163] F. Balboa Usabiaga, R. Delgado-Buscalioni, B. E. Griffith, A. Donev, *Comput. Methods Appl. Mech. Eng.* **2014**, 269, 139.
- [164] P. Ahlrichs, B. Dünweg, *J. Chem. Phys.* **1999**, 111, 8225.
- [165] S. Succi, *The Lattice Boltzmann Equation: For Fluid Dynamics and Beyond*, Oxford University Press, Oxford, New York **2001**.
- [166] S. Yasuda, R. Yamamoto, *Phys. Rev. E* **2010**, 81, 036308.
- [167] P. Koumoutsakos, *Annu. Rev. Fluid Mech.* **2005**, 37, 457.
- [168] K. M. Mohamed, A. A. Mohamad, *Microfluid Nanofluid* **2010**, 8, 283.
- [169] R. Delgado-Buscalioni, Numerical Analysis of Multiscale Computations **2012**, pp. 145–166.
- [170] W. E, B. Enquist, X. T. Li, W. Q. Ren, E. Vanden-Eijnden, *CiCP* **2007**, 2, 367.
- [171] X. Bian, M. Praprotnik in *Handbook of Materials Modeling. Volume 2 Applications: Current and Emerging Materials* (Eds.: W. Andreoni, S. Yip), Springer, Cham **2018**, p. 1.
- [172] Y. Wang, Z. Li, J. Xu, C. Yang, G. E. Karniadakis, *Soft Matter* **2019**, 15, 1747.
- [173] J. Lebowitz, P. Bergmann, *Ann. Phys.* **1957**, 1, 1.
- [174] P. Bergmann, J. Lebowitz, *Phys. Rev.* **1955**, 99, 578.
- [175] G. Ciccotti, L. Delle Site, *Soft Matter* **2019**, 15, 2114.
- [176] A. Agarwal, L. Delle Site, *Comp. Phys. Comm.* **2016**, 206, 26.
- [177] A. Agarwal, C. Clementi, L. Delle Site, *Phys.Chem.Chem.Phys.* **2017**, 19, 13030.
- [178] R. Potestio, P. Español, R. Delgado-Buscalioni, R. Everaers, K. Kremer, D. Donadio, *Phys. Rev. Lett.* **2013**, 111, 060601.
- [179] P. Español, R. Delgado-Buscalioni, R. Everaers, R. Potestio, D. Donadio, K. Kremer, *J. Chem. Phys.* **2015**, 142, 064115.
- [180] K. Kreis, R. Potestio, *J. Chem. Phys.* **2016**, 145, 044104.
- [181] M. Heidari, R. Cortes-Huerto, D. Donadio, R. Potestio, *Eur. Phys. J. Special Topics* **2016**, 225, 1505.
- [182] R. Everaers, *Eur. Phys. J. Spec. Top.* **2016**, 225, 1483.
- [183] C. Krekeler, A. Agarwal, C. Junghans, M. Praprotnik, L. Delle Site, *J. Chem. Phys.* **2018**, 149, 024104.
- [184] J. Whittaker, L. Delle Site, *Phys.Rev.Res.* **2019**, 1, 033099.
- [185] E. G. Flekkoy, R. Delgado-Buscalioni, P. V. Coveney, *Phys. Rev. E* **2005**, 72, 026703.
- [186] A. Donev, E. Vanden-Eijnden, A. L. Garcia, J. B. Bell, *Comm. Appl. Math and Comp. Sci.* **2010**, 5, 149.
- [187] F. Cornalba, T. Shardlow, J. Zimmer, *Nonlinearity* **2019**, in press, 1800025.
- [188] T. Lehmann, V. Konarovskyi, M.-K. von Renesse, Dean-Kawasaki dynamics: Ill-posedness vs. triviality, arxiv:1806.05018 technical report **2018**.
- [189] L. Delle Site, *Adv. Theory Simul.* **2018**, 1, 1800056.
- [190] M. Ali, J. Gan, X. Chen, G. Yu, Y. Zhang, M. Ellahi, A. Abdeltawab, *Chem.Eng.Res.Des.* **2018**, 129, 356.
- [191] A. W. Duster, C.-H. Wang, C. Garza, D. Miller, H. Lin, *WIREs Comp.Mol.Sci* **2017**, 7, e1310.
- [192] C. Krekeler, L. Delle Site, *Phys. Chem. Chem. Phys.* **2017**, 19, 4701.
- [193] B. Shadrack Jabes, C. Krekeler, R. Klein, L. Delle Site, *J. Chem. Phys.* **2018**, 148, 193804.
- [194] B. Shadrack Jabes, L. Delle Site, *J.Chem.Phys.* **2018**, 149, 184502.
- [195] L. Delle Site, *Comput. Phys. Commun.* **2018**, 222, 94.